J Math Chem (2012) 50:1815–1860
DOI 10.1007/s10910-012-0007-9

ORIGINAL PAPER

Stereoisograms of trigonal bipyramidal compounds: II. *RS*-stereogenicity/*RS*-stereoisomerism versus stereogenicity/stereoisomerism, leading to a revised interpretation of Berry's pseudorotation

Shinsaku Fujita

Received: 3 March 2012 / Accepted: 29 March 2012 / Published online: 18 April 2012

Abstract The stereoisogram approach (Fujita in J Org Chem 69:3158–3165, 2004, Tetrahedron 62:691–705, 2006, Tetrahedron 65:1581–1592, 2009) is applied to trigonal bipyramidal compounds, where chiral and achiral proligands are taken into consideration. After configurations of trigonal bipyramidal compounds are enumerated by using the partial-cycle-index method (Fujita in Symmetry and combinatorial enumeration in chemistry. Springer, Berlin, 1991), they are categorized into Type I–V cases according to the stereoisogram approach. The enumerated configurations are specified by configuration indices and *C/A*-descriptors, which are assigned in terms of *RS*-diastereomeric relationships, (not of enantiomeric relationships). The concept of *a multiplet of stereoisograms* is proposed to formulate the concept of *ortho-stereogenicity*, which is concerned with *ortho-diastereomeric relationships* between stereoisograms. On the other hand, the concept of *stereogenicity* (which has been used in the conventional stereochemistry) is redefined by starting from *RS*-stereogenicity and by comparing with the ortho-stereogenicity, where the stereogenicity is concerned with *diastereomeric relationships* between pairs of enantiomers. Berry's pseudorotation for isomerization of trigonal bipyramidal compounds is reinterpreted in order to cover more general cases in which chiral moieties along with achiral moieties (i.e., all of Type I–V cases) are taken into consideration. A modified Desargues-Levi graph is proposed to cover Type I–V cases. In addition, an adamantane-like graph is proposed to formulate Berry's pseudorotation on the basis of a multiplet of stereoisograms, where quadruplets of *RS*-stereoisomers occupy the nodes of the graph. Thereby, a multiplet of stereoisograms is shown to be a versatile tool to characterize stereoisomerization processes of inorganic stereochemistry in addition to those of organic stereochemistry.

S. Fujita (✉)
Shonan Institute of Chemoinformatics and Mathematical Chemistry, Kaneko 479-7, Ooimachi, Ashigara-Kami-Gun, Kanagawa-Ken, 258-0019, Japan
e-mail: shinsaku_fujita@nifty.com

Keywords Trigonal bipyramidal complex · Stereoisogram · *RS*-diastereomeric · *C/A*-descriptor · Berry's pseudorotation

1 Introduction

Stereomutation of pentavalent compounds has been widely investigated for about half a century so that various mechanisms have been proposed. Representative mechanisms are Berry's pseudorotation [1], Muetterties' mechanisms [2,3], and Ugi's turnstile rotation [4], as described in books [5,6] and reviews [7–11]. A systematic geometrical analysis of the stereomutation has been investigated by Lauterbur and Ramirez [12], who have noticed the Desargues-Levi graph for the isomerization process of Berry's pseudorotation. The Desargues-Levi graph has then attracted interests of several groups of theoretical chemists [13–16]. A group-theoretical approach has been applied to trigonal bipyramidal compounds by Randić [17,18]. More recently, Couzijn et al. [19] have convincingly demonstrated that Berry's pseudorotation is the fundamental mechanism by which interconversion of pentavalent isomers proceed, as reviewed in hilights [20]. On the other hand, the rigidity of a phosphorus center has been observed in specific cases as exemplified by isolation of optical active compounds [21–24].

From the viewpoint of the stereoisogram approach developed by us [25–32], the previous results on isomerization mechanisms described in the preceding paragraph are restricted to special cases in which achiral moieties (when detached) or atoms are considered to be ligands. In other words, cases of Type I and IV stereoisograms are taken but cases of Type II, III, and V stereoisograms are ignored if we follow the terminology of the stereoisograms. This means that the previous results (aiming unconsciously at Type I and IV cases) should be extended so as to cover more general cases in which chiral moieties along with achiral moieties (i.e., all of Type I–V cases) are taken into consideration. This extension is a main target of the present article.

To pursue the main target, we should carry out tasks to get over several barriers as follows:

1. Whether flexible or rigid, trigonal bipyramidal compounds with a given set of ligands should be presumed to take appropriate configurations fixed at a time-scale to be investigated. Among such configurations, an appropriate quadruplet of configurations should be examined by following the stereoisogram approach, so that *RS*-stereoisomers should be formulated as higher levels of categories in examining trigonal bipyramidal compounds. This task has been done in Part I of this series. Thereby, *RS*-stereogenicity and *RS*-stereoisomerism have been discussed apart from "stereogenicity" and "stereoisomerism" of the conventional stereochemistry, so that chirality and *RS*-stereogenicity are treated as independent concepts within *RS*-stereoisomerism.
2. Before we start to investigate isomerization processes between such fixed configurations or between quadruplets of *RS*-stereoisomers, enumeration of the fixed configurations should be investigated to grasp the scope of isomerization. As an application of the unit-subduced-cycle-index (USCI) approach [33], trigonal bipyramidal compounds have been enumerated by using the fixed point (FPM)

method of the USCI approach [34], where the results have restricted to trigonal bipyramidal isomers with achiral proligands only. In order to comprehend the stereochemistry of trigonal bipyramidal compounds, we should take account of chiral proligands along with achiral ones. In the present article, we will apply another method of the USCI approach, i.e., the partial-cycle-index (PCI) method [33], to the enumeration of trigonal bipyramidal compounds with both chiral and achiral proligands.

3. According to the IR-9.3.3.6 and IR-9.3.4.5 of the IUPAC recommendations 2005 [35], such fixed configurations should be specified by configuration indices and additionally *C/A*-descriptors, where the rules are based on the conventional presumption that a pair of *C/A*-descriptors is assigned to a pair of enantiomers. From the viewpoint of the stereoisogram approach, a set configuration index and a *C/A*-descriptor should be assigned to a pair of *RS*-diastereomers (not to a pair of enantiomers). This will be exemplified by using trigonal bipyramidal compounds. Thereby, we are able to give additional counterexamples to the conventional presumption.
4. The investigation on isomerization processes between such fixed configurations or between quadruplets of *RS*-stereoisomers requires a rational formulation of stereogenicity (or stereoisomerism) by starting from *RS*-stereogenicity (or *RS*-stereoisomerism). For this purpose, the concept of *a multiplet of stereoisograms* will be proposed. Thereby, stereogenicity (or more strictly speaking ortho-stereogenicity) is clarified to characterize such a multiplet of stereoisograms, while each of the stereoisograms characterizes *RS*-stereogenicity.
5. Berry's pseudorotation [1] should be extended to cover more general cases in which chiral moieties along with achiral moieties (i.e., all of Type I–V cases) are taken into consideration. It follows that Berry's pseudorotation will be formulated by using stereoisograms, where a multiplet of stereoisograms is a versatile tool to characterize stereoisomerization processes.

2 Symmetry-itemized enumeration of trigonal bipyramidal compounds

2.1 The partial-cycle-index (PCI) method

To grasp a total feature of isomerization processes, symmetry-itemized enumeration of trigonal bipyramidal compounds should be conducted first. Among the four methods supported by the USCI approach [33], i.e.,

1. the fixed-point matrix (FPM) method based on generating functions derived from subduced cycle indices (SCIs) and mark tables [36–38],
2. the PCI method based on generating functions derived from partial cycle indices (PCIs) [39,40],
3. the elementary superposition method [41], and
4. the partial superposition method [39,41],

the FPM method has once been applied to the symmetry-itemized enumeration of trigonal bipyramidal compounds [34]. Because the previous results [34] have been restricted to trigonal bipyramidal isomers with achiral proligands only, we should take

account of chiral proligands along with achiral ones in order to pursue the present targets. For the purpose of the versatility of the USCI approach, we here apply the PCI method to such extended enumeration of trigonal bipyramidal isomers with achiral and chiral proligands.

The point group $\mathbf{D}_{3h}$ has 10 subgroups up to conjugacy to provide a non-redundant set of subgroups (SSG) [34]:

$$\mathrm{SSG}_{\mathbf{D}_{3h}} = \left\{\mathbf{C}_1, \mathbf{C}_2, \mathbf{C}_s, \mathbf{C}'_s, \mathbf{C}_3, \mathbf{C}_{2v}, \mathbf{C}_{3v}, \mathbf{C}_{3h}, \mathbf{D}_3, \mathbf{D}_{3h}\right\}, \tag{1}$$

where the subgroups are aligned in the ascending order of their orders. The coset representations $\mathbf{D}_{3h}(/\mathbf{G}_i)$ ($\mathbf{G}_i \in \mathrm{SSG}_{\mathbf{D}_{3h}}$) generates the corresponding mark table, as reported in Table 5 of Ref. [42] (see also Table A.13 of [33]). For practices of calculations, the corresponding inverse matrix is also necessary, as reported in Table 6 of Ref. [42] (see also Table B.13 of [33]). In addition, the SCR table (Table 12 of Ref. [42] and Table C.13 of [33]) and the USCI-CF table (Table 2 of Ref. [34] and Table E.13 of [33]) are necessary, where the SCR is an acronym of *subduction of coset representations* and the USCI-CF is an acronym of *unit subduced cycle indices with chirality fittingness*.

Let us consider a reference skeleton **1**, the five vertices accommodate a set of five proligands selected from an inventory of proligands:

$$\mathbf{L} = \{\mathrm{a}, \mathrm{b}, \mathrm{c}, \mathrm{d}, \mathrm{e}, \mathrm{p}, \overline{\mathrm{p}}, \mathrm{q}, \overline{\mathrm{q}}\}, \tag{2}$$

where the proligands a–e are achiral and the pairs p/$\overline{\mathrm{p}}$ and q/$\overline{\mathrm{q}}$ represent enantiomeric pairs of chiral proligands when detached. The term *proligand* is used to indicates an abstract moiety having chirality/achirality only [33,43]. Thereby, trigonal bipyramidal compounds with a given constitution of achiral and/or chiral proligands are generated to exhibit point-group symmetries of $\mathrm{SSG}_{\mathbf{D}_{3h}}$ (Eq. 1). The present target is to calculate the number of trigonal bipyramidal compounds with a given constitution and a point-group symmetry. Note that trigonal bipyramidal compounds enumerated may be rigid or flexible. If flexible, they are regarded as configurations to be considered in isomerization processes.

The two axial (apical) vertices of the reference skeleton (**1**) belong to a two-membered orbit (equivalence class) governed by the coset representation $\mathbf{D}_{3h}(/\mathbf{C}_{3v})$, while the three equatorial vertices of the reference skeleton (**1**) belong to a three-membered orbit governed by the coset representation $\mathbf{D}_{3h}(/\mathbf{C}_{2v})$. The corresponding USCI-CFs of the orbits are selected from the USCI-CF table (Table 2 of Ref. [34] and Table E.13 of [33]) and collected formally into respective row vectors:

$$\mathbf{D}_{3h}(/\mathbf{C}_{3v})\text{-row of USCI-CFs}: \quad (b_1^2, b_2, a_1^2, c_2, b_1^2, a_2, a_1^2, c_2, b_2, a_2) \tag{3}$$

$$\mathbf{D}_{3h}(/\mathbf{C}_{2v})\text{-row of USCI-CFs}: \quad (b_1^3, b_1b_2, a_1c_2, a_1^3, b_3, a_1a_2, a_3, a_3, b_3, a_3), \tag{4}$$

where the sphericity indices, a_d, b_d, and c_d, correspond to d-membered homospheric, hemispheric, and enantiospheric orbits, respectively. The USCI-CFs for each subgroup appearing in these formal vectors (Eqs. 3 and 4) are multiplied to give an SCI-CF (a subduced cycle index with chirality fittingness). According to the PCI method of the

USCI approach [33], the resulting SCI-CFs for the respective subgroups of $\mathrm{SSG}_{\mathbf{D}_{3h}}$ (Eq. 1) are collected to give a formal inner product:

$$\text{SCF-CFs:} \quad (b_1^5, b_1b_2^2, a_1^3c_2, b_1^2b_3, a_1a_2^2, a_1^2a_3, c_2a_3, b_2b_3, a_2a_3) \tag{5}$$

which is regarded as a row vector and multiplied by the inverse matrix (Table 6 of Ref. [42] or Table B.13 of [33]). Thereby, a formal row vector is obtained, where its elements represent PCI-CFs (partial cycle indices with chirality fittingness) for the respective subgroups as follows:

$$\begin{aligned}
\text{PCI-CF}_{\mathbf{C}_1} &= \frac{1}{12}b_1^5 - \frac{1}{4}b_1b_2^2 - \frac{1}{3}a_1^3c_2 - \frac{1}{12}b_1^2b_3 + \frac{1}{2}a_1a_2^2 \\
&\quad + \frac{1}{4}a_1^2a_3 + \frac{1}{12}c_2a_3 + \frac{1}{4}b_2b_3 - \frac{1}{2}a_2a_3 && (6)\\
\text{PCI-CF}_{\mathbf{C}_2} &= \frac{1}{2}b_1b_2^2 - \frac{1}{2}a_1a_2^2 - \frac{1}{2}b_2b_3 + \frac{1}{2}a_2a_3 && (7)\\
\text{PCI-CF}_{\mathbf{C}_s} &= \frac{1}{2}a_1^3c_2 - \frac{1}{2}a_1a_2^2 - \frac{1}{2}a_1^2a_3 + \frac{1}{2}a_2a_3 && (8)\\
\text{PCI-CF}_{\mathbf{C}_s'} &= \frac{1}{6}a_1^3c_2 - \frac{1}{2}a_1a_2^2 - \frac{1}{6}c_2a_3 + \frac{1}{2}a_2a_3 && (9)\\
\text{PCI-CF}_{\mathbf{C}_3} &= \frac{1}{4}b_1^2b_3 - \frac{1}{4}a_1^2a_3 - \frac{1}{4}c_2a_3 - \frac{1}{4}b_2b_3 + \frac{1}{2}a_2a_3 && (10)\\
\text{PCI-CF}_{\mathbf{C}_{2v}} &= a_1a_2^2 - a_2a_3 && (11)\\
\text{PCI-CF}_{\mathbf{C}_{3v}} &= \frac{1}{2}a_1^2a_3 - \frac{1}{2}a_2a_3 && (12)\\
\text{PCI-CF}_{\mathbf{C}_{3h}} &= \frac{1}{2}c_2a_3 - \frac{1}{2}a_2a_3 && (13)\\
\text{PCI-CF}_{\mathbf{D}_3} &= \frac{1}{2}b_2b_3 - \frac{1}{2}a_2a_3 && (14)\\
\text{PCI-CF}_{\mathbf{D}_{3h}} &= a_2a_3. && (15)
\end{aligned}$$

When the ligand inventory $\mathbf{L}$ (Eq. 2) are taken into consideration, the following ligand inventory functions are obtained according to the USCI approach [33]:

$$\begin{aligned}
a_d &= \mathrm{a}^d + \mathrm{b}^d + \mathrm{c}^d + \mathrm{d}^d + \mathrm{e}^d && (16)\\
b_d &= \mathrm{a}^d + \mathrm{b}^d + \mathrm{c}^d + \mathrm{d}^d + \mathrm{e}^d + \mathrm{p}^d + \overline{\mathrm{p}}^d + \mathrm{q}^d + \overline{\mathrm{q}}^d && (17)\\
c_d &= \mathrm{a}^d + \mathrm{b}^d + \mathrm{c}^d + \mathrm{d}^d + \mathrm{e}^d + 2\mathrm{p}^{d/2}\overline{\mathrm{p}}^{d/2} + 2\mathrm{q}^{d/2}\overline{\mathrm{q}}^{d/2}, && (18)
\end{aligned}$$

which show the modes of substitution for d-membered homospheric (a_d), hemispheric (b_d), and enantiospheric (c_d) orbits.

The ligand inventory functions (Eqs. 16–18) are introduced into the PCI-CFs (Eqs. 6–15). The resulting equations are expanded to give generating functions for the respective subgroups of $\mathrm{SSG}_{\mathbf{D}_{3h}}$ (Eq. 1), e.g.,

$$
\begin{aligned}
f_{\mathbf{C}_2} = {} & \frac{1}{2}(a^4p + a^4\overline{p}) + \cdots + \frac{1}{2}(a^3p^2 + a^3\overline{p}^2) + \cdots + (a^2b^2p + a^2b^2\overline{p}) + \cdots \\
& + (a^2bp^2 + a^2b\overline{p}^2) + \cdots + \frac{1}{2}(a^2p^3 + a^2\overline{p}^3) + \cdots + (a^2p^2\overline{p} + a^2\overline{p}^2p) + \cdots \\
& + (a^2p^2\overline{q} + a^2\overline{p}^2q) + \cdots + \frac{1}{2}(ap^4 + a\overline{p}^4) + \cdots + (ap^2\overline{p}^2 + a\overline{p}^2p^2) + \cdots \\
& + (ap^2q^2 + a\overline{p}^2\overline{q}^2) + \cdots + \frac{1}{2}(p^4\overline{p} + p\overline{p}^4) + \cdots + \frac{1}{2}(p^4\overline{q} + \overline{p}^4q) + \cdots \\
& + \frac{1}{2}(p^3\overline{p}^2 + p^2\overline{p}^3) + \cdots + \frac{1}{2}(p^3q^2 + \overline{p}^3\overline{q}^2) + \cdots + (p^2\overline{p}^2q + p^2\overline{p}^2\overline{q}) + \cdots
\end{aligned} \tag{19}
$$

$$
\begin{aligned}
f_{\mathbf{C}_s} = {} & a^3b^2 + \cdots + 2a^3bc + \cdots + 2a^2b^2c + \cdots + 3a^2bcd + \cdots \\
& + a^3p\overline{p} + \cdots + 3a^2bp\overline{p} + \cdots + 6abcp\overline{p} + \cdots
\end{aligned} \tag{20}
$$

for the subgroups $\mathbf{C}_2$ and $\mathbf{C}_s$. Generating functions for the remaining subgroups of $\mathrm{SSG}_{\mathbf{D}_{3h}}$ (Eq. 1) are obtained in similar ways. The coefficient of each term in these generating functions exhibits the number of trigonal bipyramidal compounds with a constitution:

$$
a_{m_a}b_{m_b}c_{m_c}d_{m_d}e_{m_e}p_{n_p}\overline{p}_{n_{\overline{p}}}q_{n_q}\overline{q}_{n_{\overline{q}}} \quad (m_a+m_b+m_c+m_d+m_e+n_p+n_{\overline{p}}+n_q+n_{\overline{q}}=5), \tag{21}
$$

where the symbols m_a, n_p, etc. denote the numbers of proligands shown as respective subscripts. Although these numbers appear as subscripts in such constitutions as Eq. 21 according to chemical conventions, they appear as the superscripts of respective terms in generating functions (e.g., Eqs. 19 and 20) during enumeration by the PCI method.

According to the PCI method, a pair of enantiomers is counted once, while an achiral complex is counted once in the present enumeration. For example, the first term $\frac{1}{2}(a^4p + a^4\overline{p})$ appearing in the generating function $f_{\mathbf{C}_2}$ (Eq. 19) indicates the presence of an enantiomeric pair of compounds with the constitution a^4p (paired with $a^4\overline{p}$), where the fraction $\frac{1}{2}$ is multiplied in order to adjust the result as showing one pair of enantiomers. On the same line, the term $(a^2b^2p + a^2b^2\overline{p})$ appearing in the generating function $f_{\mathbf{C}_2}$ (Eq. 19) should be interpreted to be $2 \times \frac{1}{2}(a^2b^2p + a^2b^2\overline{p})$, which shows the presence of two pairs of enantiomers.

As for achiral compounds, the term $a^3p\overline{p}$ appearing in the generating function $f_{\mathbf{C}_s}$ (Eq. 20) indicates the presence of one achiral compound with the constitution $a^3p\overline{p}$, where the chiralities of p and $\overline{p}$ are compensated to give such an achiral compound.

The coefficients of the generating functions of the respective subgroups of $\mathrm{SSG}_{\mathbf{D}_{3h}}$ (Eq. 1), are summarized in Tables 1–3, where the constitution $a_{m_a}b_{m_b}c_{m_c}d_{m_d}e_{m_e}p_{n_p}\overline{p}_{n_{\overline{p}}}q_{n_q}\overline{q}_{n_{\overline{q}}}$ is represented by a partition:

$$
[m_a, m_b, m_c, m_d, m_e; n_p, n_{\overline{p}}, n_q, n_{\overline{q}}] \tag{22}
$$

where we presume $m_a \geq m_b \geq m_c \geq m_d \geq m_e \geq 0$; $n_p \geq n_{\overline{p}} \geq 0$; $n_q \geq n_{\overline{q}} \geq 0$; and $n_p \geq n_q \geq 0$ without losing generality. For example, the partition [4,1,0,0,0;0,0,0,0]

Table 1 Symmetry-itemized enumeration of trigonal bipyramidal compounds with achiral proligands only

Constitution	$\mathbf{C}_1$	$\mathbf{C}_2$	$\mathbf{C}_s$	$\mathbf{C}'_s$	$\mathbf{C}_3$	$\mathbf{C}_{2v}$	$\mathbf{C}_{3v}$	$\mathbf{C}_{3h}$	$\mathbf{D}_3$	$\mathbf{D}_{3h}$
[5,0,0,0,0;0,0,0,0]	0	0	0	0	0	0	0	0	0	1
[4,1,0,0,0;0,0,0,0]	0	0	0	0	0	1	1	0	0	0
[3,2,0,0,0;0,0,0,0]	0	0	1	0	0	1	0	0	0	1
[3,1,1,0,0;0,0,0,0]	0	0	2	1	0	0	1	0	0	0
[2,2,1,0,0;0,0,0,0]	1	0	2	0	0	2	0	0	0	0
[2,1,1,1,0;0,0,0,0]	3	0	3	1	0	0	0	0	0	0
[1,1,1,1,1;0,0,0,0]	10	0	0	0	0	0	0	0	0	0

Table 2 Symmetry-itemized enumeration of trigonal bipyramidal compounds with achiral and chiral proligands

Constitution	$\mathbf{C}_1$	$\mathbf{C}_2$	$\mathbf{C}_s$	$\mathbf{C}'_s$	$\mathbf{C}_3$	$\mathbf{C}_{2v}$	$\mathbf{C}_{3v}$	$\mathbf{C}_{3h}$	$\mathbf{D}_3$	$\mathbf{D}_{3h}$
[4,0,0,0,0;1,0,0,0]*	0	1/2	0	0	1/2	0	0	0	0	0
[3,0,0,0,0;2,0,0,0]*	1/2	1/2	0	0	0	0	0	0	1/2	0
[3,1,0,0,0;1,0,0,0]*	3/2	0	0	0	1/2	0	0	0	0	0
[3,0,0,0,0;1,1,0,0]	1	0	1	0	0	0	0	1	0	0
[2,2,0,0,0;1,0,0,0]*	2	1	0	0	0	0	0	0	0	0
[2,1,1,0,0;1,0,0,0]*	5	0	0	0	0	0	0	0	0	0
[2,1,0,0,0;2,0,0,0]*	2	1	0	0	0	0	0	0	0	0
[2,1,0,0,0;1,1,0,0]	3	0	3	1	0	0	0	0	0	0
[2,0,0,0,0;3,0,0,0]*	1/2	1/2	0	0	0	0	0	0	1/2	0
[2,0,0,0,0;2,1,0,0]*	2	1	0	0	0	0	0	0	0	0
[2,0,0,0,0;2,0,1,0]*	2	1	0	0	0	0	0	0	0	0
[2,0,0,0,0;1,1,1,0]*	5	0	0	0	0	0	0	0	0	0
[1,1,1,1,0;1,0,0,0]*	10	0	0	0	0	0	0	0	0	0
[1,1,1,0,0;2,0,0,0]*	5	0	0	0	0	0	0	0	0	0
[1,1,1,0,0;1,1,0,0]	6	0	6	2	0	0	0	0	0	0
[1,1,0,0,0;3,0,0,0]*	3/2	0	0	0	1/2	0	0	0	0	0
[1,1,0,0,0;2,1,0,0]*	5	0	0	0	0	0	0	0	0	0
[1,1,0,0,0;2,0,1,0]*	5	0	0	0	0	0	0	0	0	0
[1,1,0,0,0;1,1,1,0]*	10	0	0	0	0	0	0	0	0	0
[1,0,0,0,0;4,0,0,0]*	0	1/2	0	0	1/2	0	0	0	0	0
[1,0,0,0,0;3,1,0,0]*	3/2	0	0	0	1/2	0	0	0	0	0
[1,0,0,0,0;3,0,1,0]*	3/2	0	0	0	1/2	0	0	0	0	0
[1,0,0,0,0;2,2,0,0]	2	1	0	0	0	0	0	0	0	0
[1,0,0,0,0;2,0,2,0]*	2	1	0	0	0	0	0	0	0	0
[1,0,0,0,0;2,1,1,0]*	5	0	0	0	0	0	0	0	0	0
[1,0,0,0,0;1,1,1,1]	10	0	0	0	0	0	0	0	0	0

The values in an asterisked row should be duplicated

Table 3 Symmetry-itemized enumeration of trigonal bipyramidal compounds with chiral proligands only

Constitution	$\mathbf{C}_1$	$\mathbf{C}_2$	$\mathbf{C}_s$	$\mathbf{C}'_s$	$\mathbf{C}_3$	$\mathbf{C}_{2v}$	$\mathbf{C}_{3v}$	$\mathbf{C}_{3h}$	$\mathbf{D}_3$	$\mathbf{D}_{3h}$
[0,0,0,0,0;5,0,0,0]*	0	0	0	0	0	0	0	0	1/2	0
[0,0,0,0,0;4,1,0,0]*	0	1/2	0	0	1/2	0	0	0	0	0
[0,0,0,0,0;4,0,1,0]*	0	1/2	0	0	1/2	0	0	0	0	0
[0,0,0,0,0;3,2,0,0]*	1/2	1/2	0	0	0	0	0	0	1/2	0
[0,0,0,0,0;3,0,2,0]*	1/2	1/2	0	0	0	0	0	0	1/2	0
[0,0,0,0,0;3,1,1,0]*	3/2	0	0	0	1/2	0	0	0	0	0
[0,0,0,0,0;2,2,1,0]*	2	1	0	0	0	0	0	0	0	0
[0,0,0,0,0;2,1,1,1]*	5	0	0	0	0	0	0	0	0	0

The values in an asterisked row should be duplicated

represents a case of $m_{\mathrm{a}} = 4$ and $m_{\mathrm{b}} = 1$ ($\mathrm{a}_4\mathrm{b}$, i.e., four a's and one b), a case of $m_{\mathrm{a}} = 1$ and $m_{\mathrm{b}} = 4$ (ab_4, i.e.,one a and four b's), a case of $m_{\mathrm{b}} = 4$ and $m_{\mathrm{c}} = 1$ ($\mathrm{b}_4\mathrm{c}$, i.e., four b's and one c), a case of $m_{\mathrm{b}} = 1$ and $m_{\mathrm{c}} = 4$ (bc_4, i.e., one b and four c's), or others, because the coefficients of these cases are equal to each other. The data of Eq. 19 (or Eq. 20) appear in the $\mathbf{C}_2$-column (or the $\mathbf{C}_s$-column) of each of Tables 1–3. Each row with an asterisk gives pairs of enantiomers so that each coefficient collected should be duplicated to give the number of enantiomeric pairs. Several data collected in Table 1 (from the [5,0,0,0,0;0,0,0,0]-row to the [2,2,1,0,0;0,0,0,0]-row) are identical with the data obtained previously by using FPM method [34]. Thus, the PCI method is shown to be as versatile as the FPM method.

Table 1 shows that there appear no isomers for $\mathbf{C}_2$, $\mathbf{C}_3$, $\mathbf{C}_{3h}$, and $\mathbf{D}_3$, when only achiral proligands are taken into consideration. This fact is confirmed generally by introducing $s_d = a_d = b_d = c_d$ into the PCI-CFs for these subgroups (Eqs. 7, 10, 13, and 14), where the resulting PCIs (without chirality fittingness) vanish to zero.

3 Stereoisomeric groups and multiplets of stereoisograms

3.1 *RS*-stereoisomeric groups

Although the construction of *RS*-stereoisomeric groups by starting from the point group $\mathbf{D}_{3h}$ has been discussed in detail in Part I of this series, essential items will be introduced to develop stereoisomeric groups for comprehending stereochemical features of trigonal bipyramidal compounds.

The point group $\mathbf{D}_{3h}$ acting on a trigonal bipyramidal skeleton is characterized by the coset decomposition $\mathbf{D}_{3h} = \mathbf{D} + \sigma_h\mathbf{D}_3$, where the representative σ_h is a reflection due to the trigonal plane of the trigonal bipyramidal skeleton. Let the symbol $\widetilde{\sigma}_h$ denote be an *RS*-permutation which converts the trigonal bipyramidal skeleton having permutated ligands with no ligand inversions. Let the symbol $\widehat{I}$ be a ligand inversion which causes ligand inversions without changing the skeleton, where $\widetilde{\sigma}_h = \sigma_h\widehat{I}$. Then, the *RS*-stereoisomeric group $\mathbf{D}_{3h\widetilde{\sigma}\widehat{I}}$ is defined as follows:

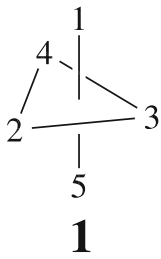

Fig. 1 Reference numbering of vertices in a trigonal bipyramidal skeleton, where a central atom is omitted. Although bonds between the central atom and respective equatorial proligands (2, 3, and 4) are omitted, the three equatorial proligands are linked with lines hypothetically to emphasize the *trigonal* plane

$$\mathbf{D}_{3h\widetilde{\sigma}\widehat{I}} = \mathbf{D}_3 + \sigma_h\mathbf{D}_3 + \widetilde{\sigma}_h\mathbf{D}_3 + \widehat{I}\mathbf{D}_3 \tag{23}$$

Because $\mathbf{D}_3$ is a normal subgroup of $\mathbf{D}_{3h\widetilde{\sigma}\widehat{I}}$, the corresponding factor group is constructed as follows:

$$\mathbf{D}_{3h\widetilde{\sigma}\widehat{I}}/\mathbf{D}_3 = \{\mathbf{D}_3, \sigma_h\mathbf{D}_3, \widetilde{\sigma}_h\mathbf{D}_3, \widehat{I}\mathbf{D}_3\}, \tag{24}$$

which is isomorphic to the Klein four-group. Obviously, the transversal of Eq. 23 gives the following group:

$$\mathbf{D}_{3h\widetilde{\sigma}\widehat{I}}/\mathbf{D}_3 \sim \{I, \sigma_h, \widetilde{\sigma}_h, \widehat{I}\}, \tag{25}$$

which is also isomorphic to the Klein four-group.

As shown above, the five vertices of a trigonal bipyramidal skeleton construct orbits governed by coset representations, $\mathbf{D}_{3h}(/\mathbf{C}_{3v})$ and $\mathbf{D}_{3h}(/\mathbf{C}_{2v})$. The coset representations can be extended to coset representations, $\mathbf{D}_{3h\widetilde{\sigma}\widehat{I}}(/\mathbf{C}_{3v\widetilde{\sigma}\widehat{I}})$ and $\mathbf{D}_{3h\widetilde{\sigma}\widehat{I}}(/\mathbf{C}_{2v\widetilde{\sigma}\widehat{I}})$, where $\mathbf{C}_{3v\widetilde{\sigma}\widehat{I}}$ and $\mathbf{C}_{2v\widetilde{\sigma}\widehat{I}}$ are generated by starting from the point groups, $\mathbf{C}_{3v}$ ($= \mathbf{C}_3 + \sigma_{v(1)}\mathbf{C}_3$) and $\mathbf{C}_{2v}$ ($= \mathbf{C}_2 + \sigma_h\mathbf{C}_2$), in a similar way to Eq. 23 (i.e., $\mathbf{D}_3$ is substituted for $\mathbf{C}_3$ or $\mathbf{C}_2$).

Following the numbering shown in Fig. 1, the transversal appearing in Eq. 25 corresponds to the following set of operations:

$$I \sim (1)(5)|(2)(3)(4) \tag{26}$$
$$\sigma_h \sim \overline{(1\ 5)|(2)(3)(4)} \tag{27}$$
$$\widetilde{\sigma}_h \sim (1\ 5)|(2)(3)(4) \tag{28}$$
$$\widehat{I} \sim \overline{(1)(5)|(2)(3)(4)}, \tag{29}$$

where disjoint cycles without and with an overbar are selected from $\mathbf{D}_{3h\widetilde{\sigma}\widehat{I}}(/\mathbf{C}_{3v\widetilde{\sigma}\widehat{I}})$ (before each vertical bar) and $\mathbf{D}_{3h\widetilde{\sigma}\widehat{I}}(/\mathbf{C}_{2v\widetilde{\sigma}\widehat{I}})$ (after each vertical bar). These operations construct a group isomorphic to the Klein four-group.

According to the stereoisogram approach [25,26,44], the action of the transversal (Eqs. 26–29) on the reference skeleton **1** (Fig. 1) generates a quadruplet of reference skeletons (**1**, $\overline{\mathbf{1}}$, **2**, and $\overline{\mathbf{2}}$), which are depicted to form a reference stereoisogram shown in Fig. 2.

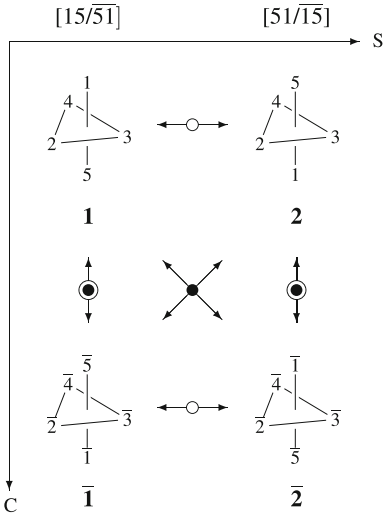

Fig. 2 Reference stereoisogram of a *trigonal* bipyramidal skeleton, which is tentatively drawn as a Type III stereoisogram. Each number with an overbar represents the accommodation of a proligand with a reflected configuration. When a pair of enantiomers is emphasized, such a notation as [15/$\overline{51}$] (or [51/$\overline{15}$]) is used by referring to the numbering of the two apical nodes

3.2 Stereogenic group for a trigonal bipyramidal skeleton

The *RS*-stereoisomeric group $\mathbf{D}_{3h\widetilde{\sigma}\widehat{I}}$ (Eq. 23) contains the *RS*-permutation group $\mathbf{D}_{3\widetilde{\sigma}}$ as a subgroup, i.e.,

$$\mathbf{D}_{3\widetilde{\sigma}} = \mathbf{D}_3 + \widetilde{\sigma}_h \mathbf{D}_3 \tag{30}$$

which is regarded as a permutation group of degree 5 ($|\mathbf{D}_{3\widetilde{\sigma}}| = 12$). The *RS*-permutation group $\mathbf{D}_{3\widetilde{\sigma}}$ is alternatively called *an RS-stereogenic group* if we later take account of a stereogenic group for a trigonal bipyramidal skeleton.

The *RS*-permutation group $\mathbf{D}_{3\widetilde{\sigma}}$ can be tentatively equalized to the sum of coset representations $\mathbf{D}_{3\widetilde{\sigma}}(/\mathbf{C}_{3\widetilde{\sigma}'}) + \mathbf{D}_{3\widetilde{\sigma}}(/\mathbf{C}_{2\widetilde{\sigma}'})$, where $\mathbf{C}_{3\widetilde{\sigma}'}$ and $\mathbf{C}_{2\widetilde{\sigma}'}$ correspond to $\mathbf{C}_{3v}$ and $\mathbf{C}_{2v}$ without considering ligand reflections (cf. Fig. 1 of Part I of this series). Because the *RS*-permutation group $\mathbf{D}_{3\widetilde{\sigma}}$ is isomorphic to $\mathbf{D}_{3h}$, the above sum of coset representations is tentatively equalized (as a group of permutations) to the sum of the coset representations $\mathbf{D}_{3h}(/\mathbf{C}_{3v}) + \mathbf{D}_{3h}(/\mathbf{C}_{2v})$ without considering ligand reflections (i.e., by the deletion of overbars, cf. Fig. 1 of Part I of this series). Following this convention, the *RS*-permutation group $\mathbf{D}_{3\widetilde{\sigma}}$ (Eq. 30) can be regarded as a subgroup of the symmetric group of degree 5 ($\mathbf{S}^{[5]}$), the order of which is calculated to be $|\mathbf{S}^{[5]}| = 5! = 120$. Because the symmetric group of degree 5 ($\mathbf{S}^{[5]}$) generates stereoisomers with no ligand reflections, it is called *a stereogenic group* for trigonal bipyramidal compounds. A coset decomposition of the symmetric group $\mathbf{S}^{[5]}$ by the *RS*-permutation group $\mathbf{D}_{3\widetilde{\sigma}}$ is calculated as follows:

$$\begin{aligned}\mathbf{S}^{[5]} = {} & \mathbf{D}_{3\widetilde{\sigma}} + (1\ 2)\mathbf{D}_{3\widetilde{\sigma}} + (1\ 3)\mathbf{D}_{3\widetilde{\sigma}} + (1\ 4)\mathbf{D}_{3\widetilde{\sigma}} \\ & + (4\ 5)\mathbf{D}_{3\widetilde{\sigma}} + (1\ 2)(4\ 5)\mathbf{D}_{3\widetilde{\sigma}} + (1\ 3)(4\ 5)\mathbf{D}_{3\widetilde{\sigma}}\end{aligned}$$

$$
\begin{aligned}
&+(3\ 5)\mathbf{D}_{3\tilde{\sigma}} + (1\ 2)(3\ 5)\mathbf{D}_{3\tilde{\sigma}} \\
&+(2\ 5)\mathbf{D}_{3\tilde{\sigma}}
\end{aligned} \tag{31}
$$

where a 1-cycle is omitted so that a shortened disjoint cycle (1 2), for example, represents a disjoint cycle (1 2)(3)(4)(5) as a full list of cycles. The number of the cosets are calculated to be $|\mathbf{S}^{[5]}|/|\mathbf{D}_{3\tilde{\sigma}}| = 120/12 = 10$.

The normalizer $N(\mathbf{D}_{3\tilde{\sigma}})$ of the *RS*-permutation group $\mathbf{D}_{3\tilde{\sigma}}$ in the symmetric group $\mathbf{S}^{[5]}$ is found to be the *RS*-permutation group $\mathbf{D}_{3\tilde{\sigma}}$ itself (this has been confirmed by using the Maple system), so that the number of conjugate subgroups of $\mathbf{D}_{3\tilde{\sigma}}$ is calculated to be $|\mathbf{S}^{[5]}|/|N(\mathbf{D}_{3\tilde{\sigma}})| = |\mathbf{S}^{[5]}|/|\mathbf{D}_{3\tilde{\sigma}}| = 120/12 = 10$. Hence, the 10 cosets appearing in the right-hand side of Eq. 31 generate respective conjugate subgroups of $\mathbf{D}_{3\tilde{\sigma}}$, which fix the corresponding cosets, e.g., a conjugate subgroup $(1\ 2)\mathbf{D}_{3\tilde{\sigma}}(1\ 2)^{-1}$ fixes the coset $(1\ 2)\mathbf{D}_{3\tilde{\sigma}}$.

3.3 Stereoisomeric group for a trigonal bipyramidal skeleton

The representatives of the cosets appearing in the right-hand side of Eq. 31 are operated onto the *RS*-stereoisomeric group $\mathbf{D}_{3h\tilde{\sigma}\hat{I}}$ (Eq. 23) so as to give a further group:

$$
\begin{aligned}
\mathbf{S}^{[5]}_{\mathbf{D}_{3h\tilde{\sigma}\hat{I}}} = {} & \mathbf{D}_{3h\tilde{\sigma}\hat{I}} + (1\ 2)\mathbf{D}_{3h\tilde{\sigma}\hat{I}} + (1\ 3)\mathbf{D}_{3h\tilde{\sigma}\hat{I}} + (1\ 4)\mathbf{D}_{3h\tilde{\sigma}\hat{I}} \\
&+(4\ 5)\mathbf{D}_{3h\tilde{\sigma}\hat{I}} + (1\ 2)(4\ 5)\mathbf{D}_{3h\tilde{\sigma}\hat{I}} + (1\ 3)(4\ 5)\mathbf{D}_{3h\tilde{\sigma}\hat{I}} \\
&+(3\ 5)\mathbf{D}_{3h\tilde{\sigma}\hat{I}} + (1\ 2)(3\ 5)\mathbf{D}_{3h\tilde{\sigma}\hat{I}} \\
&+(2\ 5)\mathbf{D}_{3h\tilde{\sigma}\hat{I}}
\end{aligned} \tag{32}
$$

which is called *the stereoisomeric group* of a trigonal bipyramidal skeleton. The order of the stereoisomeric group $\mathbf{S}^{[5]}_{\mathbf{D}_{3h\tilde{\sigma}\hat{I}}}$ is calculated to be $|\mathbf{S}^{[5]}_{\mathbf{D}_{3h\tilde{\sigma}\hat{I}}}| = |\mathbf{D}_{3h\tilde{\sigma}\hat{I}}| \times 10 = 24 \times 10 = 240$.

By referring to Eqs. 23 and 30, the *RS*-stereoisomeric group $\mathbf{D}_{3h\tilde{\sigma}\hat{I}}$ is constructed by a direct product $\mathbf{D}_{3\tilde{\sigma}} \times \{I, \sigma_h\}$. Thereby, the stereoisomeric group $\mathbf{S}^{[5]}_{\mathbf{D}_{3h\tilde{\sigma}\hat{I}}}$ can be alternatively constructed by a direct product $\mathbf{S}^{[5]} \times \{I, \sigma_h\}$, which is isomorphic to $\mathbf{S}^{[5]} \times \mathbf{S}^{[2]}$.

This mode of construction is conducted by a program of the Maple language so as to reveal that the normalizer $N(\mathbf{D}_{3h\tilde{\sigma}\hat{I}})$ of the *RS*-stereoisomeric group $\mathbf{D}_{3h\tilde{\sigma}\hat{I}}$ in the stereoisomeric group $\mathbf{S}^{[5]}_{\mathbf{D}_{3h\tilde{\sigma}\hat{I}}}$ is the $\mathbf{D}_{3h\tilde{\sigma}\hat{I}}$ group itself. Hence, the number of conjugate subgroups of the $\mathbf{D}_{3h\tilde{\sigma}\hat{I}}$ group is calculated to be

$$
\frac{|\mathbf{S}^{[5]}_{\mathbf{D}_{3h\tilde{\sigma}\hat{I}}}|}{|N(\mathbf{D}_{3h\tilde{\sigma}\hat{I}})|} = \frac{|\mathbf{S}^{[5]}_{\mathbf{D}_{3h\tilde{\sigma}\hat{I}}}|}{|\mathbf{D}_{3h\tilde{\sigma}\hat{I}}|} = \frac{240}{24} = 10. \tag{33}
$$

As a result, the 10 cosets appearing in the right-hand side of Eq. 32 generate respective conjugate subgroups of $\mathbf{D}_{3h\tilde{\sigma}\hat{I}}$, which fix the corresponding cosets, e.g., a conjugate subgroup $(1\ 2)\mathbf{D}_{3h\tilde{\sigma}\hat{I}}(1\ 2)^{-1}$ fixes the coset $(1\ 2)\mathbf{D}_{3h\tilde{\sigma}\hat{I}}$.

3.4 Multiplets of stereoisograms for a trigonal bipyramidal skeleton

The respective cosets appearing in the stereoisomeric group $\mathbf{S}^{[5]}_{\mathbf{D}_{3h\widetilde{\sigma}\widehat{I}}}$ (Eq. 32) generate a set of 10 reference stereoisograms, each of which is stereoisomeric to the original reference stereoisogram shown in Fig. 2. The set (multiplet) of the 10 reference stereoisograms is shown in Fig. 3, where the stereoisogram **11** is identical with the reference stereoisogram shown in Fig. 2, i.e., $\mathbf{1}=\mathbf{3}$, $\mathbf{2}=\mathbf{4}$, $\overline{\mathbf{1}}=\overline{\mathbf{3}}$, and $\overline{\mathbf{2}}=\overline{\mathbf{4}}$.

The 10 reference stereoisograms (**11**, **12**, **13**, etc.) shown in Fig. 3 correspond to the cosets appearing in the coset decomposition shown in Eq. 32. For example, Stereoisogram **12** corresponds to the coset $(1\ 2)\mathbf{D}_{3h\widetilde{\sigma}\widehat{I}}$ so that the reference skeleton **3** (= **1**) is converted into the reference skeletons contained in Stereoisogram **12** as follows:

$$\mathbf{3}(=\mathbf{1}) \xrightarrow{(1\ 2)} \mathbf{5} \tag{34}$$

$$\mathbf{4}(=\mathbf{2}) \xrightarrow{(1\ 2)} \mathbf{6} \quad \text{or} \quad \mathbf{3}(=\mathbf{1}) \xrightarrow[\text{via } \mathbf{4}]{(1\ 2)(1\ 5)=(1\ 5\ 2)} \mathbf{6} \tag{35}$$

$$\overline{\mathbf{3}}(=\overline{\mathbf{1}}) \xrightarrow{(1\ 2)} \overline{\mathbf{5}} \quad \text{or} \quad \mathbf{3}(=\mathbf{1}) \xrightarrow[\text{via } \overline{\mathbf{3}}]{(1\ 2)\overline{(1\ 5)}=\overline{(1\ 5\ 2)}} \overline{\mathbf{5}} \tag{36}$$

$$\overline{\mathbf{4}}(=\overline{\mathbf{2}}) \xrightarrow{(1\ 2)} \overline{\mathbf{6}} \quad \text{or} \quad \mathbf{3}(=\mathbf{1}) \xrightarrow[\text{via } \overline{\mathbf{4}}]{\overline{(1\ 2)}} \overline{\mathbf{6}} \tag{37}$$

where 1-cycles are omitted so that, for example, the symbol (1 5 2) corresponds to a product of cycles (1 5 2)(3)(4), while the symbol $\overline{(1\ 5\ 2)}$ corresponds to a product of cycles $\overline{(1\ 5\ 2)(3)(4)}$. These modes of conversions indicate that the upperleft promolecule (e.g., **5**) can be regarded as a representative of a reference stereoisogram (e.g., Stereoisogram **12**), just as the upperleft promolecule **3** (= **1**) is regarded as a representative of Stereoisogram **11**.

The 10 reference stereoisograms (**11**, **12**, **13**, etc.) shown in Fig. 3 indicate respective modes of numbering, each of which belongs to one of the conjugate subgroups described above. For example, the reference stereoisogram **12** belongs to the conjugate subgroup $(1\ 2)\mathbf{D}_{3h\widetilde{\sigma}\widehat{I}}(1\ 2)^{-1}$ corresponding to the coset $(1\ 2)\mathbf{D}_{3h\widetilde{\sigma}\widehat{I}}$. The transversal appearing in Eqs. 26–29 corresponds to the following set of operations:

$$I \sim (1\ 2)\{(1)(5)|(2)(3)(4)\}(1\ 2)^{-1} = (2)(5)|(1)(3)(4) \tag{38}$$

$$\sigma_h \sim (1\ 2)\{\overline{(1\ 5)}|(2)(3)(4)\}(1\ 2)^{-1} = \overline{(2\ 5)|(1)(3)(4)} \tag{39}$$

$$\widetilde{\sigma}_h \sim (1\ 2)\{(1\ 5)|(2)(3)(4)\}(1\ 2)-1 = (2\ 5)|(1)(3)(4) \tag{40}$$

$$\widehat{I} \sim (1\ 2)\{\overline{(1)(5)|(2)(3)(4)}\}(1\ 2)^{-1} = \overline{(2)(5)|(1)(3)(4)}, \tag{41}$$

which are contained in the conjugate subgroup $(1\ 2)\mathbf{D}_{3h\widetilde{\sigma}\widehat{I}}(1\ 2)^{-1}$. The operations represented by Eqs. 38–41 correspond to the reference skeletons **5**, $\overline{\mathbf{5}}$, **6**, and $\overline{\mathbf{6}}$, when we start from **5**.

The 10 reference stereoisograms shown in Fig. 3 are categorized in terms of reference axes (i.e., pairs of two axial vertices). Thus, each column of Fig. 3 collects reference stereoisograms which have the corresponding representative with a common

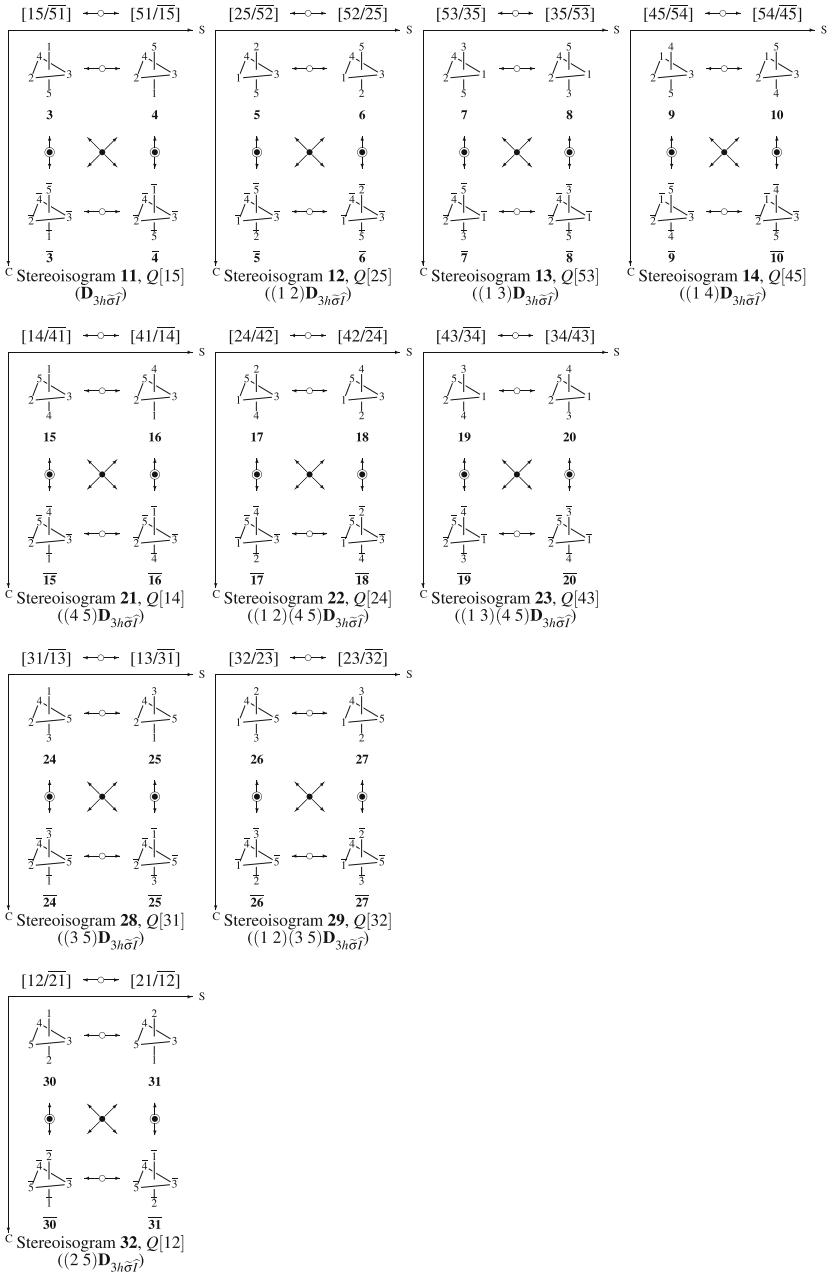

Fig. 3 Multiplet of 10 reference stereoisograms for giving trigonal bipyramidal compounds. A pair of digits and its overlined counterpart (e.g., [15/$\overline{51}$] for the pair of **3**/$\overline{\mathbf{3}}$) represent a pair of enantiomers, where the corresponding apical numbers are collected to give each pair of digits, so that the view from the first number (e.g., 1) to the second one (e.g., 5) assures the anticlockwise order of the equatorial numbering (e.g., 2–3–4). The notation $Q[v_1\,v_2]$ indicates a stereoisogram in which a representative promolecule at the *upperleft* position of the stereoisogram, where the view from the number of the first apical vertex (v_1) to that of the second one (v_2) assures the anticlockwise order of the equatorial numbering

numbering at a top vertex. For example, the first column of Fig. 3 is characterized by a common axial (apical) vertex numbered as 1 (at the top). On the other hand, each row collects reference stereoisograms which have the corresponding representative with a common numbering at a bottom vertex. For example, the first row of Fig. 3 is characterized by a common axial (apical) vertex numbered as 5 (at the bottom).

4 Terminology

As found in Ref. [45, page 58] for inorganic stereochemistry as well as in Refs. [46, page 53] and [47, pages 32–33] for organic stereochemistry, the conventional terms "stereogenicity" and "stereoisomerism" are not so well differentiated, because reflection operations and *RS*-permutations are not differentiated even when chiral and achiral ligands are taken into consideration. Before we examine trigonal bipyramidal compounds, we will briefly discuss the terminology used in the stereoisogram approach.

4.1 The terms *stereogenic* and *diastereomeric*

As found in Fig. 3, we are able to adopt two-step examinations of trigonal bipyramidal compounds:

1. At the first step, we discuss chirality and *RS*-stereogenicity by considering a stereoisogram (i.e., **11**, **12**, **13**, or others), because a quadruplet of *RS*-stereoisomers contained in such a stereoisogram is concerned with rotations and reflections (for chirality) and *RS*-permutations (for *RS*-stereogenicity).
2. At the second step, we discuss relationships among the 10 reference stereoisograms, which are convertible by means of permutations of $\mathbf{S}^{[5]}$ (Eq. 31) without reflections.

Because the relationship between any two of the 10 reference stereoisograms can be discussed apart from their inner properties (e.g., chirality and *RS*-stereogenicity), they are referred to as being *ortho-diastereomeric* if we take account of the stereogenic group $\mathbf{S}^{[5]}$ (Eq. 31). To treat cases of stereogenic groups other than $\mathbf{S}^{[5]}$, this specific case is generalized as follows:

Definition 1 (*Ortho-stereogenic and Ortho-diastereomeric*) The relational term *ortho-diastereomeric* refers to a relationship *between inequivalent stereoisograms* of the same constitution under the action of a stereogenic group (e.g., $\mathbf{S}^{[5]}$ of Eq. 31). The attributive term *ortho-stereogenic* is used if there appears such an ortho-diastereomeric relationship between a stereoisogram and any other stereoisogram.

Note that the original specification of Def. 1 is concerned with stereoisograms. In other words, Def. 1 is concerned with quadruplets of *RS*-stereoisomers, where each quadruplet is an entity to be considered. For example, when we consider trigonal bipyramidal compounds of a constitution [Mabcde], we say that Stereoisograms **11** and **12** are in an ortho-diastereomeric relationship; that Stereoisogram **11** is ortho-diastereomeric to Stereoisogram **13**; that a quadruplet for Stereoisogram **11** is an ortho-diastereomer of a quadruplet for Stereoisogram **13**; and so on. Stereoisogram

11 is ortho-stereogenic, because it has ortho-diastereomers such as **12**, **13**, etc., as shown in in Fig. 3.

If a pair of enantiomeric promolecules contained in a stereoisogram and a pair of enantiomeric promolecules contained in another stereoisogram are convertible under $\mathbf{S}^{[5]}$ (Eq. 31), they are regarded as being ortho-diastereomeric. For example, we can say that a pair of enantiomers **3/$\bar{3}$** with a constitution [Mabcde] (in Stereoisogram **11**) is ortho-diastereomeric to a pair of enantiomers **5/$\bar{5}$** with a constitution [Mabcde] (in Stereoisogram **12**).

The term *ortho-diastereomeric* can be used if a promolecule contained in a stereoisogram is converted to a promolecule contained in another stereoisogram under $\mathbf{S}^{[5]}$ (Eq. 31). For example, we can say that a promolecule **3** with a constitution [Mabcde] (in Stereoisogram **11**) is ortho-diastereomeric to a promolecule **5** with a constitution [Mabcde] (in Stereoisogram **12**). This usage is not recommended because it causes some confusion.

On the other hand, the terms *RS-stereogenic* and *RS-diastereomeric* are also used to characterize promolecules contained in a stereoisogram or to characterize pairs of enantiomers in a stereoisogram.

Definition 2 (*RS-stereogenic and RS-diastereomeric*) The relational term *RS-diastereomeric* refers to inequivalency within a stereoisogram under the action of an *RS*-permutation group (e.g., $\mathbf{D}_{3\tilde{\sigma}}$ of Eq. 30). The attributive term *RS-stereogenic* is used if there appears such an *RS*-diastereomeric relationship in the stereoisogram.

To harmonize the stereoisogram approach with the conventional stereochemistry, new definitions of the terms *stereogenic* and *diastereomeric* is provided in place of the conventional terms "stereogenic" and "diastereomeric".

Definition 3 (*Stereogenic and Diastereomeric*) The relational term *diastereomeric* refers to a relationship *between inequivalent pairs of enantiomers* (or achiral promolecules) with the same constitution under the action of the stereogenic group (e.g., $\mathbf{S}^{[5]}$ of Eq. 31). The attributive term *stereogenic* is used if there appears such an ortho-diastereomeric relationship between a pair of enantiomers and any other pair of enantiomers.

Definition 3 implicitly requires Def. 1 and Def. 2, because the *stereogenicity* (or the *diastereomeric* relationship) due to Def. 3 may coincide either with the *ortho-stereogenic* (or the *ortho-diastereomeric* relationship) due to Def. 1 or with the *RS-stereogenic* (or the *RS-diastereomeric* relationship) due to Def. 2. The latter case is important to treat chirality, which is discussed by means of a stereoisogram.

4.2 The terms *stereoisomerism* and *stereoisomeric*

If we take account of inequivalent stereoisograms under the stereoisomeric group $\mathbf{S}^{[5]}_{\mathbf{D}_{3h\tilde{\sigma}\hat{I}}}$ (Eq. 32), the relationship between any two of the 10 reference stereoisograms (Fig. 3) is referred to as being *stereoisomeric*. If the trigonal bipyramidal complex is capable of generating stereoisomeric stereoisograms, the capability (attribute) is

referred to as being *stereoisomerous* [30]. Note that the term *stereoisomerous* is an attributive term corresponding to the relational term *stereoisomeric*, just as the attributive term *RS-stereogenic* corresponds to the relational term *RS-diastereomeric* (Def. 3). In a parallel way, an attributive term *RS-stereoisomerous* should be coined to be harmonized with the relational term *RS-stereoisomeric*. Thereby, the phenomena of being stereoisomerous is referred to by the term *stereoisomerism*, just as the phenomena of being *RS*-stereoisomerous is referred to by the term *RS-stereoisomerism*.

5 Stereoisomers of trigonal bipyramidal compounds

5.1 Trigonal bipyramidal compounds with achiral proligands

Derivation of trigonal bipyramidal compounds is formulated to be substitution of a set of proligands on the vertices of reference stereoisograms shown in Fig. 3, where the mode of substitution is specified in terms of a function which determines a proligand to be placed on each vertex. When we take account of achiral proligands only, the resulting stereoisograms belong to Type I or IV. Stereoisograms of other types (Type II, III, and V) do not appear.

5.1.1 Trigonal bipyramidal compounds with five different achiral proligands ([Mabcde])

Suppose that five achiral proligands of different kinds (a, b, c, d, and e) are placed on the five vertices of the reference trigonal bipyramidal skeleton **1** (the same as **3** in Fig. 3), where the substitution mode is represented by the following function:

$$f_1 : \quad f_1(1) = \mathrm{a},\ f_1(2) = \mathrm{b},\ f_1(3) = \mathrm{c},\ f_1(4) = \mathrm{d},\ f_1(5) = \mathrm{e}, \tag{42}$$

This substitution mode may be selected otherwise without losing generality, so long as the constitution is not changed. The function f_1 is applied to the 10 reference stereoisograms shown in Fig. 3, where the central metal (M) is omitted and where we place $\overline{\mathrm{a}} = \mathrm{a}$, $\overline{\mathrm{b}} = \mathrm{b}$, $\overline{\mathrm{c}} = \mathrm{c}$, $\overline{\mathrm{d}} = \mathrm{d}$, and $\overline{\mathrm{e}} = \mathrm{e}$, because these proligands are achiral in isolation (when detached). In the present article, a letter or number with an overbar represents a mirror image of its original letter or number, whether the letter or number denotes a proligand or promolecule.

The resulting 10 stereoisograms of Type I (Fig. 4) correspond to 10 quadruplets of *RS*-stereoisomers, each of which is degenerated to a pair of enantiomers. The number 10 is consistent to the [1,1,1,1,1;0,0,0,0]-row of Table 1, where each enantiomeric pair is counted once and belongs to the point group $\mathbf{C}_1$.

As found in Fig. 4, trigonal bipyramidal compounds with the constitution [Mabcde] give 10 quadruplets of *RS*-stereoisomers, all of which are characterized as Type I. Each quadruplet is degenerated into a pair of enantiomers. As a result, there appear 10 pairs of enantiomers. According to Def. 1, each stereoisogram shown in Fig. 4 is ortho-stereogenic. Any pair of such stereoisograms (e.g., Stereoisogram **41** vs. Stereoisogram **42**) are ortho-diastereomeric. According to Def. 2, each stereoisogram shown in Fig. 4

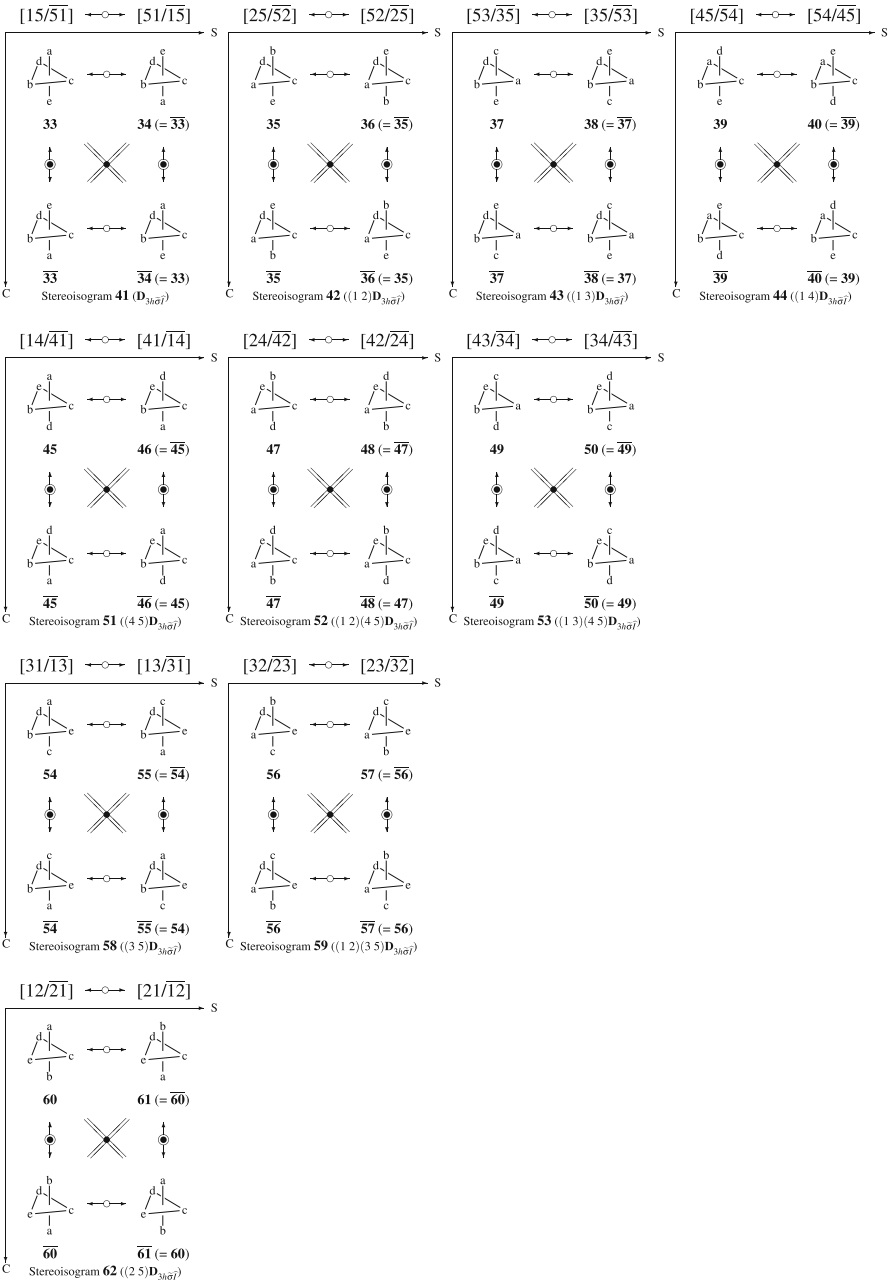

Fig. 4 Multiplet of stereoisograms for representing 10 stereoisomers (enantiomeric pairs) of trigonal bipyramidal compounds with [Mabcde]. See the [1,1,1,1,1;0,0,0,0,0]-row of Table 1. *The CIP priority* a > b > c > d > e. The central atom M is omitted

(belonging to Type I) is *RS*-stereogenic, so that it contains a pair of *RS*-diastereomers, which coincides with a pair of enantiomers.

According to Def. 3, each pair of enantiomers (e.g., **33**/$\overline{\mathbf{33}}$) in a stereoisogram of Type I is stereogenic, so as to give a pair of enantiomers (e.g., **34**/$\overline{\mathbf{34}}$), which is diastereomeric (but equivalent) to the original pair of enantiomers (e.g., **33**/$\overline{\mathbf{33}}$). Note that the equivalency stems from $\overline{\mathbf{33}} = \mathbf{34}$. Thus, chirality (providing such an enantiomeric pair) and stereogenicity (strictly speaking, *RS*-stereogenicity due to Def. 2) coincide with each other in such a stereoisogram of Type I. Note that the chirality for such a Type I case is preferred rather than the stereogenicity, which is nullified in the conventional stereochemistry.

On the other hand, a pair of enantiomers (e.g., **33**/$\overline{\mathbf{33}}$) in a stereoisogram and a pair of enantiomers (e.g., **35**/$\overline{\mathbf{35}}$) in another stereoisogram are diastereomeric according to Def. 3 so that each of the pairs of enantiomers is stereogenic according to Def 3 (strictly speaking, ortho-stereogenic due to Def. 1).

According to the IR-9.3.3.6 and IR-9.3.4.5 of the IUPAC recommendations 2005 [35], a configuration index and an *C/A*-descriptor are assigned to each pair of *RS*-diastereomers (not to a pair of enantiomers) which is contained in each of the 10 stereoisograms collected in Fig. 4, where the CIP priority is presumed to be a > b > c > d > e.

$$\left.\begin{array}{ll} \mathbf{33} & \textit{TBPY-5-15-A} \\ \mathbf{34}(=\overline{\mathbf{33}}) & \textit{TBPY-5-15-C} \end{array}\right\} (\mathbf{C}_1)\ \text{Stereoisogram } \mathbf{41}\ (\mathbf{D}_{3h\tilde{\sigma}\hat{I}})\ \text{(Type I)} \tag{43}$$

$$\left.\begin{array}{ll} \mathbf{35} & \textit{TBPY-5-25-A} \\ \mathbf{36}(=\overline{\mathbf{35}}) & \textit{TBPY-5-25-C} \end{array}\right\} (\mathbf{C}_1)\ \text{Stereoisogram } \mathbf{42}\ ((1\ 2)\mathbf{D}_{3h\tilde{\sigma}\hat{I}})\ \text{(Type I)} \tag{44}$$

$$\left.\begin{array}{ll} \mathbf{37} & \textit{TBPY-5-35-C} \\ \mathbf{38}(=\overline{\mathbf{37}}) & \textit{TBPY-5-35-A} \end{array}\right\} (\mathbf{C}_1)\ \text{Stereoisogram } \mathbf{43}\ ((1\ 3)\mathbf{D}_{3h\tilde{\sigma}\hat{I}})\ \text{(Type I)} \tag{45}$$

$$\left.\begin{array}{ll} \mathbf{39} & \textit{TBPY-5-45-A} \\ \mathbf{40}(=\overline{\mathbf{39}}) & \textit{TBPY-5-45-C} \end{array}\right\} (\mathbf{C}_1)\ \text{Stereoisogram } \mathbf{44}\ ((1\ 4)\mathbf{D}_{3h\tilde{\sigma}\hat{I}})\ \text{(Type I)} \tag{46}$$

$$\left.\begin{array}{ll} \mathbf{45} & \textit{TBPY-5-14-A} \\ \mathbf{46}(=\overline{\mathbf{45}}) & \textit{TBPY-5-14-C} \end{array}\right\} (\mathbf{C}_1)\ \text{Stereoisogram } \mathbf{51}\ ((4\ 5)\mathbf{D}_{3h\tilde{\sigma}\hat{I}})\ \text{(Type I)} \tag{47}$$

$$\left.\begin{array}{ll} \mathbf{47} & \textit{TBPY-5-24-A} \\ \mathbf{48}(=\overline{\mathbf{47}}) & \textit{TBPY-5-24-C} \end{array}\right\} (\mathbf{C}_1)\ \text{Stereoisogram } \mathbf{52}\ ((1\ 2)(4\ 5)\mathbf{D}_{3h\tilde{\sigma}\hat{I}})\ \text{(Type I)} \tag{48}$$

$$\left.\begin{array}{ll} \mathbf{49} & \textit{TBPY-5-34-C} \\ \mathbf{50}(=\overline{\mathbf{49}}) & \textit{TBPY-5-34-A} \end{array}\right\} (\mathbf{C}_1)\ \text{Stereoisogram } \mathbf{53}\ ((1\ 3)(4\ 5)\mathbf{D}_{3h\tilde{\sigma}\hat{I}})\ \text{(Type I)} \tag{49}$$

$$\left.\begin{array}{ll} \mathbf{54} & \textit{TBPY-5-13-C} \\ \mathbf{55}(=\overline{\mathbf{54}}) & \textit{TBPY-5-13-A} \end{array}\right\} (\mathbf{C}_1)\ \text{Stereoisogram } \mathbf{58}\ ((3\ 5)\mathbf{D}_{3h\tilde{\sigma}\hat{I}})\ \text{(Type I)} \tag{50}$$

$$\left.\begin{array}{ll} \mathbf{56} & \textit{TBPY-5-23-C} \\ \mathbf{57}(=\overline{\mathbf{56}}) & \textit{TBPY-5-23-A} \end{array}\right\} (\mathbf{C}_1)\ \text{Stereoisogram } \mathbf{59}\ ((1\ 2)(3\ 5)\mathbf{D}_{3h\tilde{\sigma}\hat{I}})\ \text{(Type I)} \tag{51}$$

$$\left.\begin{array}{ll} \mathbf{60} & \textit{TBPY-5-12-A} \\ \mathbf{61}(=\overline{\mathbf{60}}) & \textit{TBPY-5-12-C} \end{array}\right\} (\mathbf{C}_1)\ \text{Stereoisogram } \mathbf{62}\ ((2\ 5)\mathbf{D}_{3h\tilde{\sigma}\hat{I}})\ \text{(Type I)} \tag{52}$$

According to the stereoisogram approach, a pair of *C/A*-descriptors is given to a pair of *RS*-diastereomers, but not to a pair of enantiomers, so that the *C/A*-descriptors assigned originally to such an *RS*-diastereomeric pair is reinterpreted to be assigned to an enantiomeric pair in terms of chirality-faithful [31]. The CIP priority of temporary mirror-image proligands $\overline{a} > \overline{b} > \overline{c} > \overline{d} > \overline{e} > \overline{f}$ is obtained to be equal to the CIP priority of the original ligands, i.e., $a > b > c > d > e > f$. This means that all the cases of Fig. 4 are chirality-faithful [31]. Hence, the *C/A*-descriptor assigned to each pair of *RS*-diastereomers (Eqs. 43–52) can be regarded as being assigned to a pair of enantiomers.

5.1.2 Trigonal bipyramidal compounds with [Ma_2bcd]

Suppose that five achiral proligands of four kinds (2a, b, c, and d) are placed on the five vertices of the reference trigonal bipyramidal skeleton **1** (the same as **3** in Fig. 3), where the substitution mode is represented by the following function:

$$f_2: \quad f_2(1) = a,\ f_2(2) = b,\ f_2(3) = c,\ f_2(4) = d,\ f_2(5) = a, \tag{53}$$

This substitution mode may be selected otherwise without losing generality, so long as the constitution is not changed. The function f_1 is applied to the 10 reference stereoisograms shown in Fig. 3, where the central atom (M) is omitted and where we place $\overline{a} = a, \overline{b} = b, \overline{c} = c$, and $\overline{d} = d$, because these proligands are achiral in isolation (when detached). The resulting 10 stereoisograms (Fig. 5) exhibit several sets of coincidence in accord with the above-mentioned result of combinatorial enumeration, which shows the presence of three achiral promolecules of $\mathbf{C}_s$, one achiral promolecule of $\mathbf{C}'_s$, and three pairs of enantiomers of $\mathbf{C}_1$ (the [2,1,1,1,0;0,0,0,0]-row of Table 1).

The three achiral promolecules of $\mathbf{C}_s$ correspond to the stereoisograms of Type IV, i.e., Stereoisogram **79**, **80**, and **85** shown in Fig. 5. In each of these stereoisograms of Type IV, a quadruplet of *RS*-stereoisomers is degenerated into a single achiral promolecule, i.e., **76**, **77**, or **83**, which is characterized by the following configuration index according to the IR-9.3.3.6 of the IUPAC recommendations 2005 [35]:

76 *TBPY-5-24* ($\mathbf{C}_s$) Stereoisogram **79** ((1 2)(4 5)$\mathbf{D}_{3h\tilde{\sigma}\hat{I}}$) (Type IV) (54)

77 *TBPY-5-34* ($\mathbf{C}_s$) Stereoisogram **80** ((1 3)(4 5)$\mathbf{D}_{3h\tilde{\sigma}\hat{I}}$) (Type IV) (55)

83 *TBPY-5-23* ($\mathbf{C}_s$) Stereoisogram **85** ((1 2)(3 5)$\mathbf{D}_{3h\tilde{\sigma}\hat{I}}$) (Type IV) (56)

The $\mathbf{C}_s$-promolecules (**76**, **77**, and **83**) are *RS*-astereogenic (or *RS*-non-stereogenic) because of Type IV stereoisograms. On the other hand, the presence of Stereoisogram **79**, **80**, and **85** indicates that the $\mathbf{C}_s$-promolecules (**76**, **77**, and **83**) are ortho-stereogenic according to Def. 1. They can be referred to as being stereogenic (Def. 3), although they are not *RS*-stereogenic (Def. 2). Note that each of these achiral promolecules is regarded as being self-enantiomeric in the application of Def. 3, so as to be treated formally as "a pair of self-enantiomers" in the conceptually same level of "a pair of enantiomers".

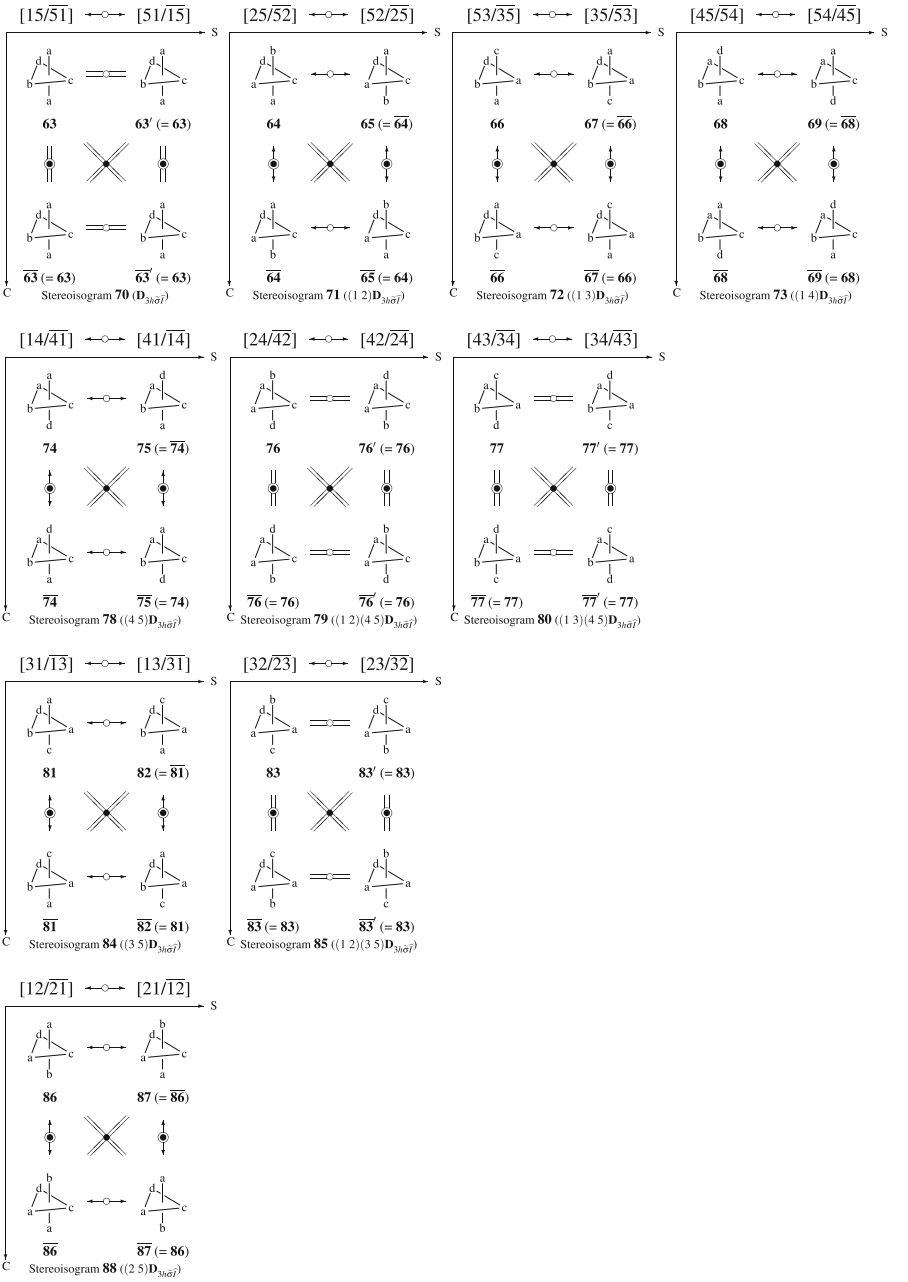

Fig. 5 Multiplet of 10 stereoisograms for representing stereoisomers (enantiomeric pairs) of trigonal bipyramidal compounds with [Ma_2bcd], i.e., three achiral promolecules of $\mathbf{C}_s$, one achiral promolecule of $\mathbf{C}'_s$, and three pairs of enantiomers of $\mathbf{C}_1$. See the -[2,1,1,1,0;0,0,0,0]-row of Table 1. *Coincidence* Stereoisogram **71** ∼ **88** (Type I for $\mathbf{C}_1$), Stereoisogram **72** ∼ **84** (Type I for $\mathbf{C}_1$), and Stereoisogram **73** ∼ **78** (Type I for $\mathbf{C}_1$). *The CIP priority* a > b > c > d. The central atom M is omitted

One achiral promolecule of $\mathbf{C}'_s$ is represented by the formula **63**, which corresponds to Stereoisogram **70** of Type IV, as shown in Fig. 5. The $\mathbf{C}'_s$-promolecule is characterized by the following configuration index according to the IR-9.3.3.6 of the IUPAC recommendations 2005 [35]:

$$\textbf{63}\ \textit{TBPY-5-11}\ \ (\mathbf{C}'_s)\ \text{Stereoisogram}\ \textbf{70}\ (\mathbf{D}_{3h\tilde{\sigma}\hat{1}})\ \text{(Type IV)} \tag{57}$$

The presence of ortho-diastereomeric $\mathbf{C}_s$-promolecules with the constitution [Ma_2bcd] (**76**, **77**, and **83**) allows us to say that the $\mathbf{C}'_s$-promolecule **63** with the same constitution [Ma_2bcd] is ortho-stereogenic (Def. 1) and stereogenic (Def. 3), although it is not *RS*-stereogenic (Def. 2).

Each of the three enantiomeric pairs of chiral $\mathbf{C}_1$-promolecules corresponds to a set of two stereoisograms of Type I, i.e., Stereoisogram **71** $\sim$ **88** (or Stereoisograms **72** $\sim$ **84**, or Stereoisograms **73** $\sim$ **78**), which are equivalent under the action of a subgroup of the stereoisomeric group.

According to the IR-9.3.3.6 and IR-9.3.4.5 of the IUPAC recommendations 2005 [35], a configuration index with a *C/A*-descriptor is assigned to a pair of *RS*-diastereomers (not to a pair of enantiomers), where the CIP priority is presumed to be a > b > c > d.

$$\left.\begin{array}{ll}\textbf{64} & \textit{TBPY-5-12-C}\\ \textbf{65}(=\overline{\textbf{64}}) & \textit{TBPY-5-12-A}\end{array}\right\}\ (\mathbf{C}_1)\ \text{Stereoisogram}\ \textbf{71}\ ((1\ 2)\mathbf{D}_{3h\tilde{\sigma}\hat{1}})\ \text{(Type I)} \tag{58}$$

(equivalent to Stereoisogram **88**)

$$\left.\begin{array}{ll}\textbf{66} & \textit{TBPY-5-13-A}\\ \textbf{67}(=\overline{\textbf{66}}) & \textit{TBPY-5-13-C}\end{array}\right\}\ (\mathbf{C}_1)\ \text{Stereoisogram}\ \textbf{72}\ ((1\ 3)\mathbf{D}_{3h\tilde{\sigma}\hat{1}})\ \text{(Type I)} \tag{59}$$

(equivalent to Stereoisogram **84**)

$$\left.\begin{array}{ll}\textbf{68} & \textit{TBPY-5-14-C}\\ \textbf{69}(=\overline{\textbf{68}}) & \textit{TBPY-5-14-A}\end{array}\right\}\ (\mathbf{C}_1)\ \text{Stereoisogram}\ \textbf{73}\ ((1\ 4)\mathbf{D}_{3h\tilde{\sigma}\hat{1}})\ \text{(Type I)} \tag{60}$$

(equivalent to Stereoisogram **78**)

These $\mathbf{C}_1$-promolecules of Type I (Fig. 5) can be discussed in a similar way to the cases of Fig. 4. Hence, *RS*-stereogenicity (and *RS*-diastereomeric relationships) as well as ortho-stereogenicity (and ortho-diastereomeric relationships) are assigned to the $\mathbf{C}_1$-promolecules of Type I (Fig. 5).

5.1.3 Trigonal bipyramidal compounds with [Ma_2b_2c]

Five achiral proligands of three kinds (2a, 2b, and c) are placed on the five vertices of the reference trigonal bipyramidal skeleton **1** (the same as **3** in Fig. 3), where the substitution mode is represented by the following function:

$$f_3:\quad f_3(1)=\mathrm{a},\ f_3(2)=\mathrm{b},\ f_3(3)=\mathrm{b},\ f_3(4)=\mathrm{c},\ f_3(5)=\mathrm{a}, \tag{61}$$

This substitution mode may be selected otherwise without losing generality, so long as the constitution [Ma_2b_2c] is not changed. The function f_3 is applied to the 10 reference

stereoisograms shown in Fig. 3, where the central atom (M) is omitted and where we place $\overline{a} = a$, $\overline{b} = b$, and $\overline{c} = c$, because these proligands are achiral in isolation (when detached). The resulting 10 stereoisograms (Fig. 6) exhibit several sets of coincidence in accord with the above-mentioned result of combinatorial enumeration, which shows the presence of two achiral promolecules of $\mathbf{C}_{2v}$, two achiral promolecules of $\mathbf{C}_s$, and one pair of enantiomers of $\mathbf{C}_1$ (the partition-[2,2,1,0,0;0,0,0,0]-row of Table 1).

The two promolecules of $\mathbf{C}_{2v}$ correspond to the stereoisograms of Type IV, i.e., Stereoisograms **95** and **109** (Fig. 6), where each quadruplet of *RS*-stereoisomers is degenerated into a single achiral promolecule, i.e., **89** or **107**. They are characterized by the following configuration indices according to the IR-9.3.3.6 of the IUPAC recommendations 2005 [35]:

$$\textbf{89}\ \textit{TBPY-5-11}\ (\mathbf{C}_{2v})\ \text{Stereoisogram}\ \textbf{95}\ (\mathbf{D}_{3h\widetilde{\sigma}\widehat{I}})\ \text{(Type IV)} \tag{62}$$

$$\textbf{107}\ \textit{TBPY-5-22}\ (\mathbf{C}_{2v})\ \text{Stereoisogram}\ \textbf{109}\ ((1\ 2)(3\ 5)\mathbf{D}_{3h\widetilde{\sigma}\widehat{I}})\ \text{(Type IV)} \tag{63}$$

The two achiral promolecule of $\mathbf{C}_s$ correspond to stereoisograms of Type IV, which have equivalent stereoisograms under the action of the stereoisomeric group. Thus, Stereoisogram **98** is equivalent to Stereoisogram **102**, while Stereoisogram **103** is equivalent to Stereoisogram **104**. These $\mathbf{C}_s$-promolecules are characterized by the following configuration indices according to the IR-9.3.3.6 of the IUPAC recommendations 2005 [35]:

$$\textbf{94}\ \textit{TBPY-5-13}\ (\mathbf{C}_s)\ \text{Stereoisogram}\ \textbf{98}\ ((1\ 4)\mathbf{D}_{3h\widetilde{\sigma}\widehat{I}})\ \text{(Type IV)}\ \text{(equivalent to Stereoisogram}\ \textbf{102}\text{)} \tag{64}$$

$$\textbf{100}\ \textit{TBPY-5-23}\ (\mathbf{C}_s)\ \text{Stereoisogram}\ \textbf{103}\ ((1\ 2)(4\ 5)\mathbf{D}_{3h\widetilde{\sigma}\widehat{I}})\ \text{(Type IV)}\ \text{(equivalent to Stereoisogram}\ \textbf{104}\text{)} \tag{65}$$

The $\mathbf{C}_{2v}$-promolecules (**89** and **107**) characterized by Eqs. 62 and 63 as well as the $\mathbf{C}_s$-promolecules (**94** and **100**) characterized by Eqs. 64 and 65 are *RS*-astereogenic (or *RS*-non-stereogenic) because they are contained in Type IV stereoisograms (Def. 2). On the other hand, the Type IV stereoisograms at issue are ortho-diastereomeric to one another according to Def. 1, so that these achiral promolecules are ortho-stereogenic (Def. 1) as well as stereogenic (Def. 3).

The one pair of chiral enantiomers of $\mathbf{C}_1$ corresponds to a set of four stereoisograms of Type I, i.e., Stereoisogram **96** $\sim$ **97** $\sim$ **108** $\sim$ **112**, which are equivalent under the action of the stereoisomeric group.

According to the IR-9.3.3.6 and IR-9.3.4.5 of the IUPAC recommendations 2005 [35], a configuration index with a *C/A*-descriptor is assigned to a pair of *RS*-diastereomers (not to a pair of enantiomers), where the CIP priority is presumed to be a > b > c.

$$\left.\begin{array}{ll}\textbf{90} & \textit{TBPY-5-12-C}\\ \textbf{91}(=\overline{\textbf{90}}) & \textit{TBPY-5-12-A}\end{array}\right\}\ (\mathbf{C}_1)\ \text{Stereoisogram}\ \textbf{96}\ ((1\ 2)\mathbf{D}_{3h\widetilde{\sigma}\widehat{I}})\ \text{(Type I)}\ \text{(equivalent to Stereoisograms}\ \textbf{97}\text{,}\ \textbf{108}\text{, and}\ \textbf{112}\text{)} \tag{66}$$

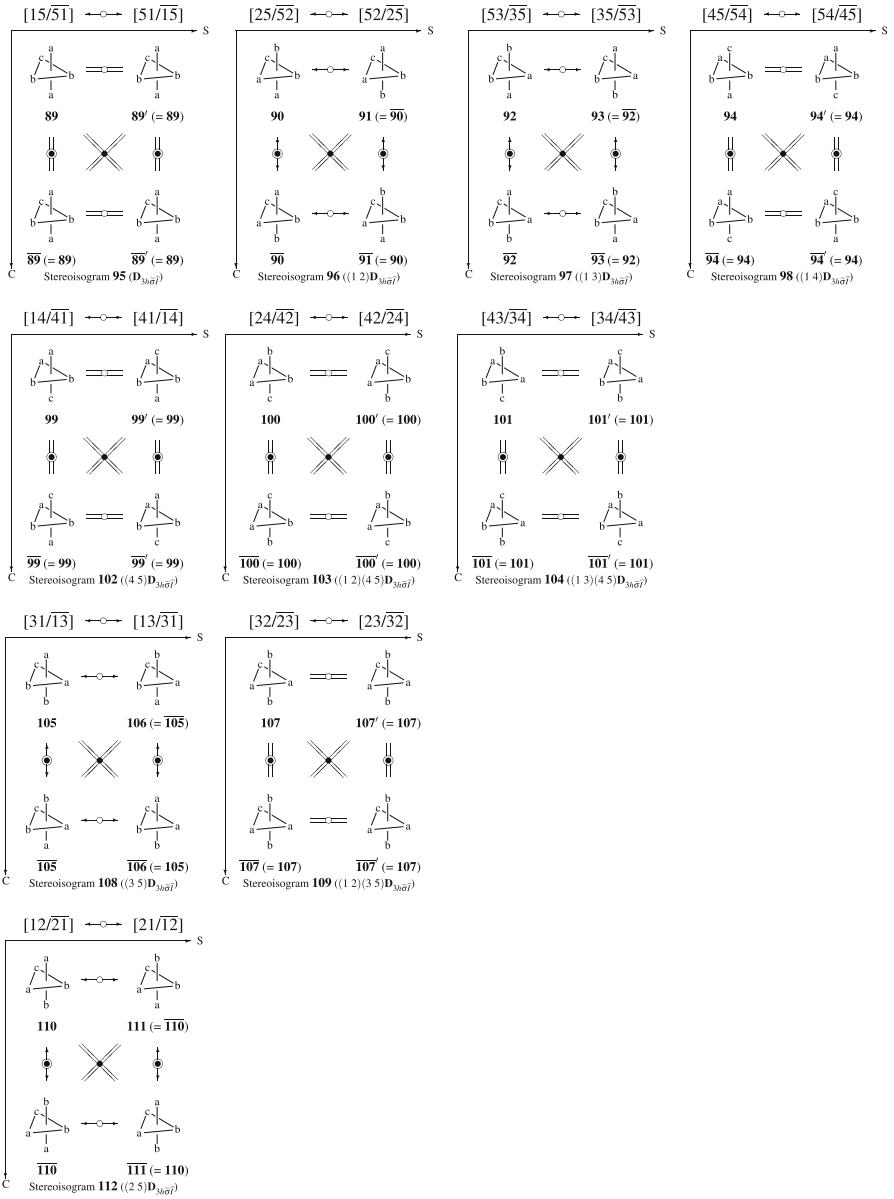

Fig. 6 Multiplet of 10 stereoisograms for representing stereoisomers (enantiomeric pairs) of trigonal bipyramidal compounds with $[Ma_2b_2c]$, i.e., two achiral promolecule of $\mathbf{C}_{2v}$, two achiral promolecules of $\mathbf{C}_s$, and one pair of enantiomers of $\mathbf{C}_1$. See the [2,2,1,0,0;0,0,0,0]-row of Table 1. *Coincidence* Stereoisogram **96** ∼ **97** ∼ **108** ∼ **112** (Type I for $\mathbf{C}_1$), Stereoisogram **98** ∼ **102** (Type IV for $\mathbf{C}_s$), and Stereoisogram **103** ∼ **104** (Type IV for $\mathbf{C}_s$). *The CIP priority* a > b > c. The central atom M is omitted

The $\mathbf{C}_1$-promolecule of Type I (Fig. 6) can be discussed in a similar way to the cases of Fig. 4. Hence, *RS*-stereogenicity (and *RS*-diastereomeric relationships) as

well as ortho-stereogenicity (and ortho-diastereomeric relationships) are assigned to the $\mathbf{C}_1$-promolecules of Type I (Fig. 6).

5.1.4 Trigonal bipyramidal compounds with achiral ligands of other constitutions

When we consider only achiral proligands as substituents, resulting promolecules belong to Type IV (achiral) or Type I (chiral). If they belong to Type IV, they are *RS*-astereogenic (or *RS*-non-stereogenic) under the action of the *RS*-permutation group (or the *RS*-stereogenic group, i.e., $\mathbf{D}_{3\tilde{\sigma}}$), while they are ortho-stereogenic under the action of the stereogenic group $\mathbf{S}^{[5]}$ (Eq. 31). If resulting chiral promolecules belong to Type I, they are *RS*-stereogenic and ortho-stereogenic.

Compounds with [Ma_3bc] Trigonal bipyramidal compounds with the constitution [Ma_3bc] are generated by placing five achiral proligands of three kinds (3a, b, and c) on the five vertices of the reference trigonal bipyramidal skeleton **1** (the same as **3** in Fig. 3). The substitution mode is represented by the following function:

$$f_4: \quad f_4(1) = \mathrm{b},\ f_4(2) = \mathrm{a},\ f_4(3) = \mathrm{a},\ f_4(4) = \mathrm{a},\ f_4(5) = \mathrm{c}, \tag{67}$$

which is applied to the 10 reference stereoisograms shown in Fig. 3.

The resulting 10 stereoisograms suffer from redundancy due to equivalency. Among them, representatives without redundancy are depicted in Fig. 7 in accord with the result of the [3,1,1,0,0;0,0,0,0]-row of Table 1, i.e., one achiral promolecule of $\mathbf{C}_{3v}$, two achiral promolecules of $\mathbf{C}_s$, and one achiral promolecule of $\mathbf{C}'_s$.

Because all of the achiral promolecules shown in Fig. 7 are contained in Type IV stereoisograms (Def. 2), they are not *RS*-stereogenic (i.e., *RS*-astereogenic). On the other hand, the Type IV stereoisograms at issue are ortho-diastereomeric to one another according to Def. 1, so that these achiral promolecules are ortho-stereogenic (Def. 1) as well as stereogenic (Def. 3).

According to the IR-9.3.3.6 of the IUPAC recommendations 2005 [35], a configuration index is given to each promolecule as shown at the bottom of each stereoisogram, where the CIP priority is presumed to be a > b > c.

Compounds with [Ma_3b_2] As for trigonal bipyramidal compounds with [Ma_3b_2], five achiral proligands of two kinds (3a and 2b) are placed on the five vertices of the reference trigonal bipyramidal skeleton **1** (the same as **3** in Fig. 3), where the substitution mode is represented by the following function:

$$f_5: \quad f_5(1) = \mathrm{b},\ f_5(2) = \mathrm{a},\ f_5(3) = \mathrm{a},\ f_5(4) = \mathrm{a},\ f_5(5) = \mathrm{b}, \tag{68}$$

which is applied to the 10 reference stereoisograms shown in Fig. 3.

Among the resulting 10 stereoisograms, representatives are depicted in Fig. 8 in accord with the result of the [3,2,0,0,0;0,0,0,0]-row of Table 1, i.e., one achiral promolecule of $\mathbf{D}_{3h}$, one achiral promolecules of $\mathbf{C}_{2v}$, and one achiral promolecule of $\mathbf{C}_s$.

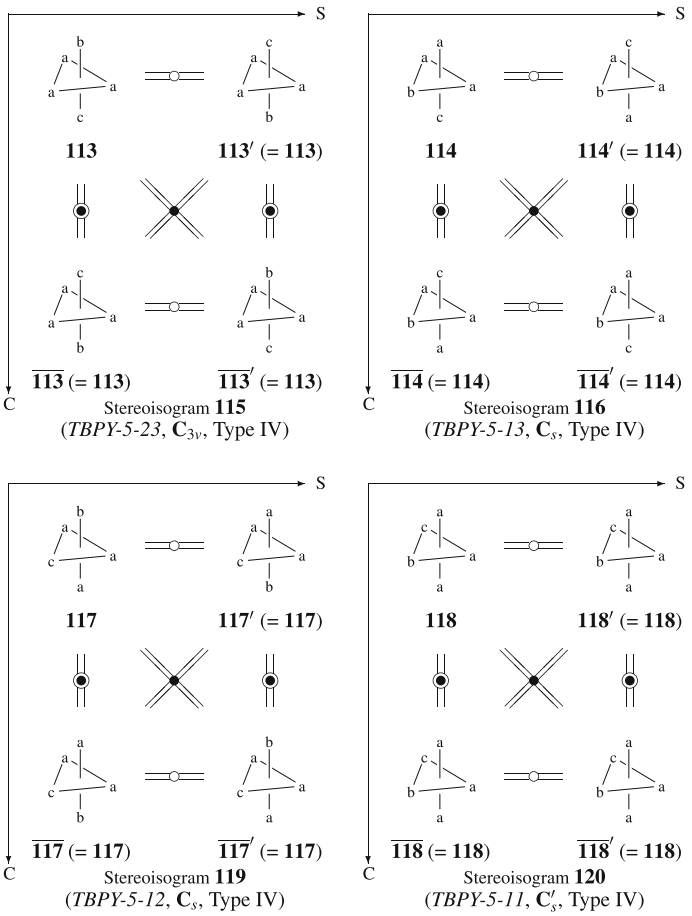

Fig. 7 Stereoisomers of trigonal bipyramidal compounds with [Ma_3bc], i.e., one achiral promolecule of $\mathbf{C}_{3v}$, two achiral promolecules of $\mathbf{C}_s$, and one achiral promolecule of $\mathbf{C}'_s$. See the [3,1,1,0,0;0,0,0,0,0]-row of Table 1. *The CIP priority* a > b > c. The central atom M is omitted

All of the achiral promolecules shown in Fig. 8 are characterized by Type IV stereoisograms, so that they are *RS*-astereogenic (or *RS*-non-stereogenic) in terms of Def. 2. On the other hand, the Type IV stereoisograms at issue are ortho-diastereomeric to one another according to Def. 1, so that these achiral promolecules are ortho-stereogenic (Def. 1) as well as stereogenic (Def. 3).

According to the IR-9.3.3.6 of the IUPAC recommendations 2005 [35], a configuration index is assigned to each promolecule as shown at the bottom of each stereoisogram, where the CIP priority is presumed to be a > b.

Compounds with [Ma_4b] To generate trigonal bipyramidal compounds with [Ma_4b], five achiral proligands (4a and b) are placed on the five vertices of the reference trigonal bipyramidal skeleton **1** (the same as **3** in Fig. 3). The substitution mode is represented by the following function:

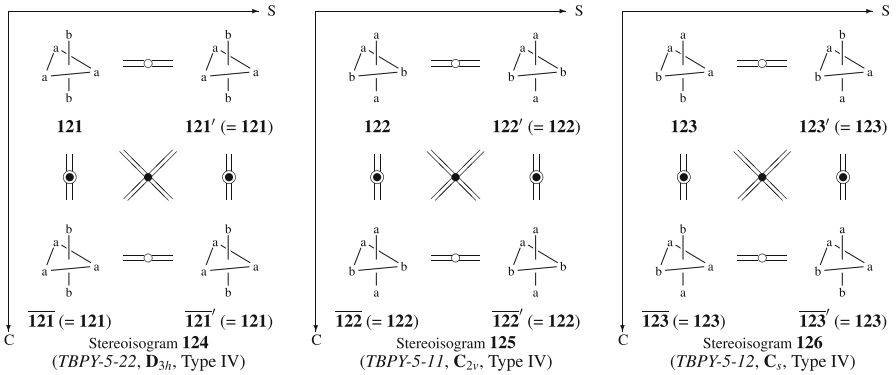

Fig. 8 Stereoisomers of trigonal bipyramidal compounds with [Ma_3b_2], i.e., one achiral promolecule of $\mathbf{D}_{3h}$, one achiral promolecules of $\mathbf{C}_{2v}$, and one achiral promolecule of $\mathbf{C}_s$. See the [3,2,0,0,0;0,0,0,0]-row of Table 1. *The CIP priority* a > b. The central atom M is omitted

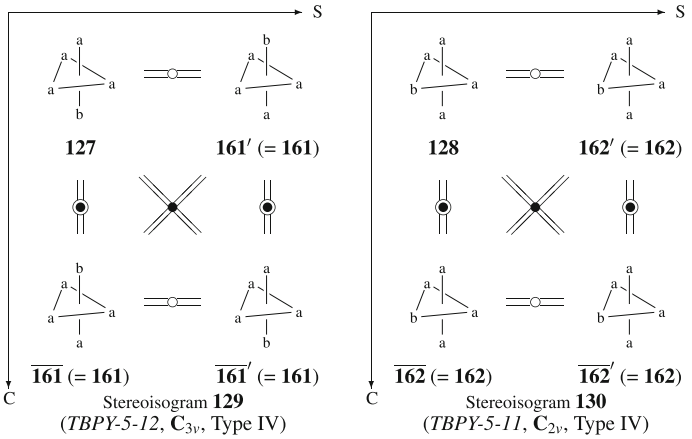

Fig. 9 Stereoisomers of trigonal bipyramidal compounds with [Ma_4b], i.e., one achiral promolecule of $\mathbf{C}_{3v}$ and one achiral promolecules of $\mathbf{C}_{2v}$. See the [4,1,0,0,0;0,0,0,0]-row of Table 1. *The CIP priority* a > b. The central atom M is omitted

$$f_6: \quad f_6(1) = \mathrm{a},\ f_6(2) = \mathrm{a},\ f_6(3) = \mathrm{a},\ f_6(4) = \mathrm{a},\ f_6(5) = \mathrm{b}, \tag{69}$$

which is applied to the 10 reference stereoisograms shown in Fig. 3.

Among the resulting 10 stereoisograms, representatives are depicted in Fig. 9 in accord with the result of the [4,1,0,0,0;0,0,0,0]-row of Table 1, i.e., one achiral promolecules of $\mathbf{C}_{3v}$ and one achiral promolecule of $\mathbf{C}_{2v}$.

Because all of the achiral promolecules shown in Fig. 9 are contained in Type IV stereoisograms, they are *RS*-astereogenic (or *RS*-non-stereogenic) according to Def. 2. On the other hand, the Type IV stereoisograms at issue are ortho-diastereomeric to one another according to Def. 1, so that these achiral promolecules are ortho-stereogenic (Def. 1) as well as stereogenic (Def. 3).

According to the IR-9.3.3.6 of the IUPAC recommendations 2005 [35], a configuration index is assigned to each promolecule as shown at the bottom of each stereoisogram, where the CIP priority is presumed to be a > b.

Compounds with [Ma_5] One achiral promolecule with [Ma_5] belongs to $\mathbf{D}_{3h}$, as reported in the [5,0,0,0,0;0,0,0,0]-row of Table 1. This promolecule is *RS*-astereogenic (Def. 2), ortho-astereogenic (Def. 1), and astereogenic (Def. 3) so as to give no stereoisomers. The corresponding stereoisogram exhibits a Type IV character, although it is omitted.

5.2 Trigonal bipyramidal compounds with chiral and achiral proligands

In this subsection, we take account of chiral proligands as substituents along with achiral proligands, where stereoisograms of Type II, III, and V are generated so as to exhibit more-complicated features. These cases have been overlooked or exceptionally treated in the conventional inorganic stereochemistry.

5.2.1 Trigonal bipyramidal compounds with [Mabcp$\overline{\text{p}}$]

Consider a set of three achiral proligands (a, b, and c) and a pair of enantiomeric chiral proligands (p and $\overline{\text{p}}$) to generate trigonal bipyramidal compounds with [Mabcp$\overline{\text{p}}$]. The set of proligands is placed on the five vertices of the reference trigonal bipyramidal skeleton **1** (the same as **3** in Fig. 3), where the substitution mode is represented by the following function:

$$f_7: \quad f_7(1) = \text{p},\ f_7(2) = \text{a},\ f_7(3) = \text{b},\ f_7(4) = \text{c},\ f_7(5) = \overline{\text{p}}. \tag{70}$$

After this function is applied to the 10 reference stereoisograms shown in Fig. 3, the resulting 10 stereoisograms (Fig. 10) are examined from a viewpoint of equivalence under the stereoisomeric group. They are categorized into equivalence classes in accord with the result of the [1,1,1,0,0;1,1,0,0]-row of Table 2. Thereby, we are able to confirm the presence of six achiral promolecules of $\mathbf{C}_s$, two achiral promolecules of $\mathbf{C}'_s$, and six pairs of enantiomeric promolecules of $\mathbf{C}_1$.

The six promolecules of $\mathbf{C}_s$ construct three stereoisograms of Type V, i.e., **150**, **151**, and **157** of Fig. 10, each of which contains a degenerate pair of *RS*-diastereomers as follows:

145 *TBPY-5-13-c*
146 *TBPY-5-13-a*
} ($\mathbf{C}_s$) Stereoisogram **150** ((1 2)(4 5)$\mathbf{D}_{3h\tilde{\sigma}\hat{I}}$) (Type V) (71)

147 *TBPY-5-23-a*
148 *TBPY-5-23-c*
} ($\mathbf{C}_s$) Stereoisogram **151** ((1 3)(4 5)$\mathbf{D}_{3h\tilde{\sigma}\hat{I}}$) (Type V) (72)

154 *TBPY-5-12-a*
155 *TBPY-5-12-c*
} ($\mathbf{C}_s$) Stereoisogram **157** ((1 2)(3 5)$\mathbf{D}_{3h\tilde{\sigma}\hat{I}}$) (Type V). (73)

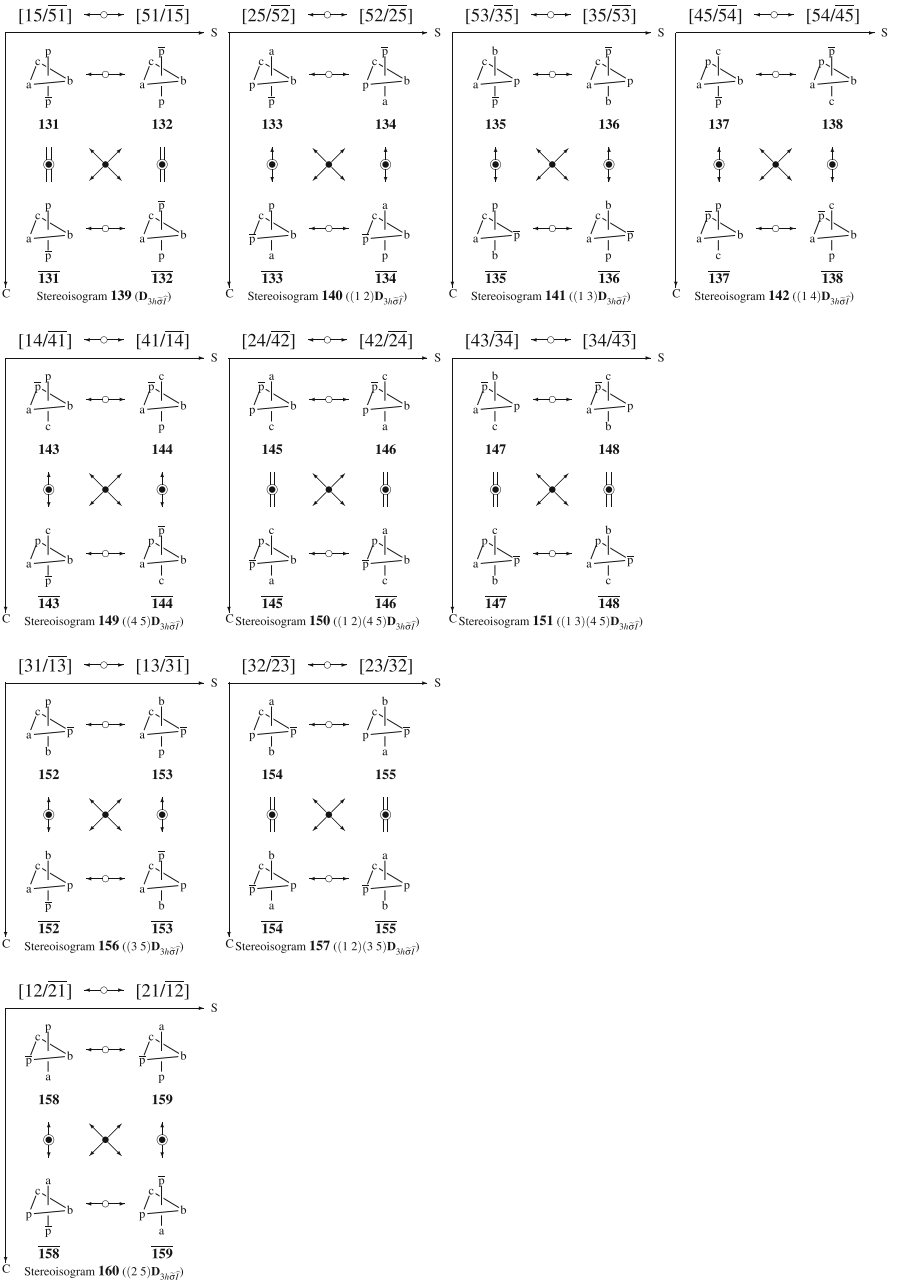

Fig. 10 Multiplet of 10 stereoisograms for representing stereoisomers (enantiomeric pairs) of trigonal bipyramidal compounds with [Mabcp$\overline{\text{p}}$], i.e., six achiral promolecule of $\mathbf{C}_s$, two achiral promolecules of $\mathbf{C}'_s$, and six pairs of enantiomers of $\mathbf{C}_1$. See the [1,1,1,0,0;1,1,0,0]-row of Table 2. *Coincidence* Stereoisogram **140** $\sim$ **160** (Type III for $\mathbf{C}_1$), Stereoisogram **141** $\sim$ **156** (Type III for $\mathbf{C}_1$), and Stereoisogram **142** $\sim$ **149** (Type III for $\mathbf{C}_1$). *The CIP priority* a > b > c > p > $\overline{\text{p}}$. The central atom M is omitted

Similarly, two promolecules of $\mathbf{C}'_s$ are contained in a single stereoisogram of Type V, i.e., Stereoisogram **139**, as found in the top of Fig. 10. The quadruplet of Stereoisogram **139** is degenerated into the following pair of *RS*-diastereomers:

$$\left.\begin{array}{l}\mathbf{131}\ \textit{TBPY-5-45-a}\\ \mathbf{132}\ \textit{TBPY-5-45-c}\end{array}\right\}\ (\mathbf{C}'_s)\ \text{Stereoisogram}\ \mathbf{139}\ (\mathbf{D}_{3h\widetilde{\sigma}\widehat{I}})\ (\text{Type V}) \tag{74}$$

The configuration indices shown in Eqs. 71–74 are assigned by presuming the CIP priority a > b > c > p > $\overline{\text{p}}$ according to the IR-9.3.3.6 of the IUPAC recommendations 2005 [35].

As found in Eqs. 71–74, *C/A*-descriptors are pairwise assigned to each pair of the *RS*-diastereomers, where the naming of *C/A*-descriptors is conducted according to the IR-9.3.4.5 of the IUPAC recommendations 2005 [35]. Because the promolecules characterized by Type V stereoisograms are achiral, the results of Eqs. 71–74 indicate that such a pair of *C/A*-descriptors due to the IR-9.3.4.6 of the IUPAC recommendations 2005 [35] by no means differentiate an enantiomeric relationship, which is absent in each of the achiral promolecules characterized by Eqs. 71–74 as well as between them. Hence, lowercase letters (*c* and *a*) are given because no existence of enantiomeric counterparts indicates a chirality unfaithful situation according to the chirality-faithfulness discussed in Ref. [31].

The six pairs of chiral promolecules of $\mathbf{C}_1$ are characterized by three stereoisograms of Type III, i.e., Stereoisograms **140**, **141**, and **142**, which exhibit the following coincidence: Stereoisogram **140** ∼ **160**, Stereoisogram **141** ∼ **156**, and Stereoisogram **142** ∼ **149**. According to the IR-9.3.3.6 and IR-9.3.4.5 of the IUPAC recommendations 2005 [35], a pair of configuration indices with a *C/A*-descriptor is assigned to a pair of *RS*-diastereomers (not to a pair of enantiomers) as follows:

$$\left.\begin{array}{l}\mathbf{133}\ \textit{TBPY-5-15-A}\\ \mathbf{134}\ \textit{TBPY-5-15-C}\\ \overline{\mathbf{133}}\ \textit{TBPY-5-14-C}\\ \overline{\mathbf{134}}\ \textit{TBPY-5-14-A}\end{array}\right\}\ (\mathbf{C}_1)\ \text{Stereoisogram}\ \mathbf{140}\ ((1\ 2)\mathbf{D}_{3h\widetilde{\sigma}\widehat{I}})\ (\text{Type III}) \tag{75}$$

(equivalent to Stereoisogram **160**)

$$\left.\begin{array}{l}\mathbf{135}\ \textit{TBPY-5-25-C}\\ \mathbf{136}\ \textit{TBPY-5-25-A}\\ \overline{\mathbf{135}}\ \textit{TBPY-5-24-A}\\ \overline{\mathbf{136}}\ \textit{TBPY-5-24-C}\end{array}\right\}\ (\mathbf{C}_1)\ \text{Stereoisogram}\ \mathbf{141}\ ((1\ 3)\mathbf{D}_{3h\widetilde{\sigma}\widehat{I}})\ (\text{Type III}) \tag{76}$$

(equivalent to Stereoisogram **156**)

$$\left.\begin{array}{l}\mathbf{137}\ \textit{TBPY-5-35-A}\\ \mathbf{138}\ \textit{TBPY-5-35-C}\\ \overline{\mathbf{137}}\ \textit{TBPY-5-34-C}\\ \overline{\mathbf{138}}\ \textit{TBPY-5-34-A}\end{array}\right\}\ (\mathbf{C}_1)\ \text{Stereoisogram}\ \mathbf{142}\ ((1\ 4)\mathbf{D}_{3h\widetilde{\sigma}\widehat{I}})\ (\text{Type III}) \tag{77}$$

(equivalent to Stereoisogram **149**)

The present stereoisogram approach is based on a theoretical foundation different from the conventional stereochemistry, although the practices of giving the

C/A-descriptors are done according to the IR-9.3.3.4 and IR-9.3.4.8 of the IUPAC recommendations 2005 [35]. For example, Eq. 75 indicates that the *RS*-diastereomers **133/134** are considered to be pairwise named, i.e., *TBPY-5-15-A* for **133** and *TBPY-5-15-C* for **134**, where the CIP priority is presumed to be $a > b > c > p > \overline{p}$. Note that the configuration indices (*TBPY-5-15* for both **133** and **134**) are identical with each other and that the *C/A*-descriptors, i.e., *A* of **133** and *C* of **134**, are paired rationally in terms of the stereoisogram approach.

In contrast, if we obey the conventional stereochemistry, we are forced to name a pair of enantiomers **133**/$\overline{\mathbf{133}}$ to give *TBPY-5-15-A* for **133** and *TBPY-5-14-C* for $\overline{\mathbf{133}}$. Obviously, the resulting names are not paired because the configuration indices, i.e., *TBPY-5-15* for **133** and *TBPY-5-14* for $\overline{\mathbf{133}}$, are not identical with each other, even though the *C/A*-descriptors, i.e., *A* of **133** and *C* of $\overline{\mathbf{133}}$, are seemingly paired. Note that the configuration indices and the *C/A*-descriptors stem from the same CIP priority (i.e., $a > b > c > p > \overline{p}$).

In the enumeration by the USCI approach (Tables 1–3), a pair of enantiomers is counted once, just as an achiral promolecule is counted one. Hence, the two *RS*-diastereomers contained in a stereoisogram of Type V are counted separately to give two stereoisomers, so that the three stereoisograms of Type V, i.e., **150**, **151**, and **157**, indicate the presence of six promolecules of $\mathbf{C}_s$, which is consistent with the value at the intersection between the $\mathbf{C}_s$-column and the [1,1,1,0,0;1,1,0,0]-row of Table 2. Similarly, the one stereoisogram of Type V, i.e., **139**, indicates the presence of two promolecules of $\mathbf{C}'_s$, which is also consistent with the value at the intersection between the $\mathbf{C}'_s$-column and the [1,1,1,0,0;1,1,0,0]-row of Table 2. Moreover, the three stereoisograms of Type III, i.e., **140**, **141**, and **142**, indicate the presence of six pairs of enantiomers of $\mathbf{C}_1$-symmetry, where the value 6 is again consistent with the value at the intersection between the $\mathbf{C}_1$-column and the [1,1,1,0,0;1,1,0,0]-row of Table 2.

5.2.2 Trigonal bipyramidal compounds with [Mabcp$_2$] *or* [Mabc$\overline{\text{p}}_2$]

Let us examine three achiral proligands (a, b, and c) and two chiral proligands (2p or 2$\overline{\text{p}}$) as a set of substituents for the five vertices of the reference trigonal bipyramidal skeleton **1** (the same as **3** in Fig. 3), where p and $\overline{\text{p}}$ represent enantiomeric proligands of a pair. Then, the substitution mode is represented by the following function:

$$f_8: \quad f_8(1) = \text{p},\ f_8(2) = \text{a},\ f_8(3) = \text{b},\ f_8(4) = \text{c},\ f_8(5) = \text{p}, \tag{78}$$

which is applied to the 10 reference stereoisograms shown in Fig. 3. The resulting 10 stereoisograms (Fig. 11) coincide to generate promolecules as equivalence classes under the action of the stereoisomeric group.

The value 5 at the intersection between the $\mathbf{C}_1$-column and the [1,1,1,0,0;2,0,0,0]-row of Table 2 implies the same value 5 for the counterpart partition [1,1,1,0,0;0,2,0,0] though omitted. It follows that this value should be duplicated to be interpreted so as to be $10 \times \frac{1}{2}(\text{abcp}^2 + \text{abc}\overline{\text{p}}^2)$, which indicates the presence of 10 pairs of enantiomers of $\mathbf{C}_1$-symmetry. This calculation is confirmed by Fig. 11, where four stereoisograms of Type II (each corresponding to one pair of enantiomers) and three stereoisograms of Type III (each corresponding to two pairs of enantiomers) are effective to characterize

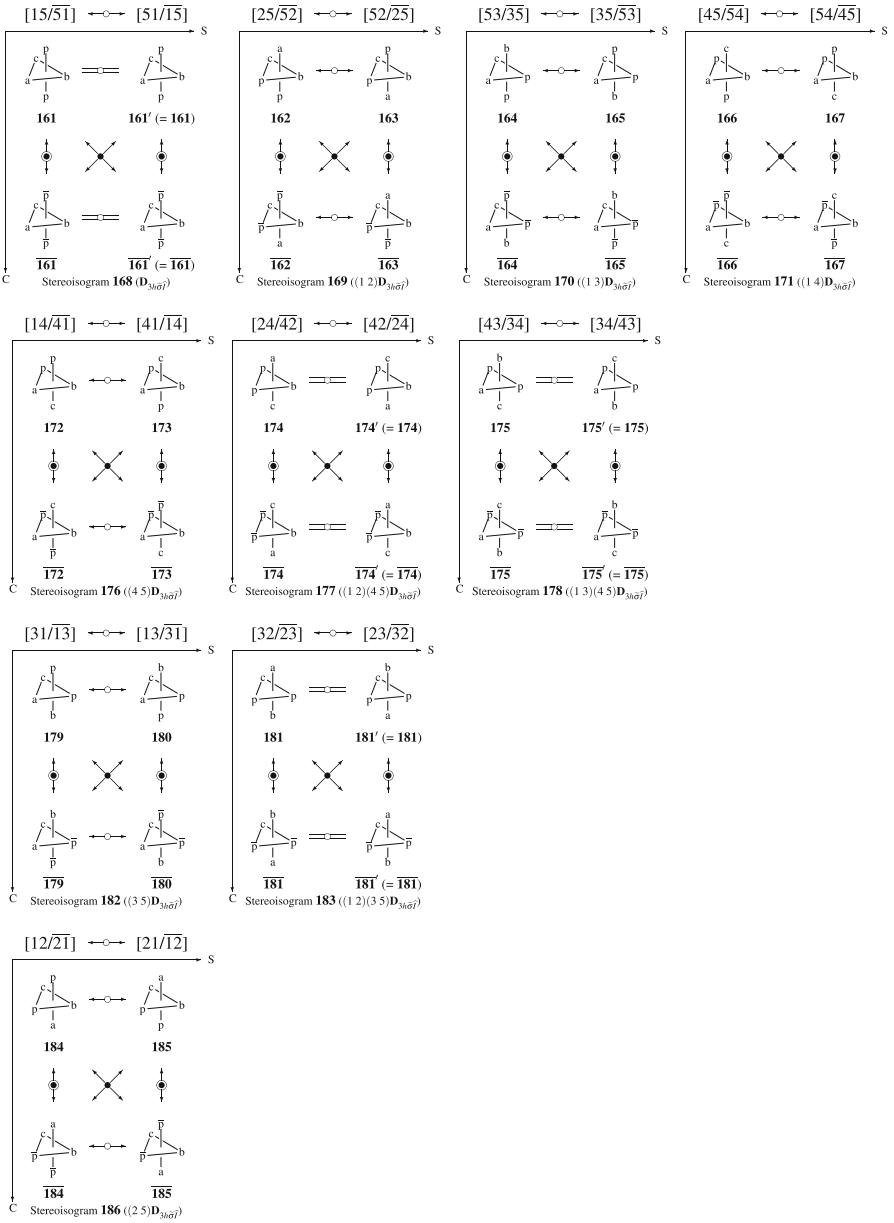

Fig. 11 Multiplet of 10 stereoisograms for representing stereoisomers (enantiomeric pairs) of trigonal bipyramidal compounds with [Mabcp$_2$] or [Mabc$\overline{\text{p}}_2$], i.e., ten pairs of enantiomers of $\mathbf{C}_1$. See the [1,1,1,0,0;2,0,0,0]-row of Table 2. *Coincidence* Stereoisogram **169** $\sim$ **186** (Type III for $\mathbf{C}_1$), Stereoisogram **170** $\sim$ **182** (Type III for $\mathbf{C}_1$), and Stereoisogram **171** $\sim$ **176** (Type III for $\mathbf{C}_1$). *The CIP priority* a > b > c > p > $\overline{\text{p}}$. The central atom M is omitted

the generated promolecules so as to show the number of pairs of enantiomers to be $4 + 3 \times 2 = 10$.

The four pairs of enantiomeric chiral promolecules of $\mathbf{C}_1$ are represented by stereoisograms of Type II, i.e., **168**, **177**, **178**, and **183** of Fig. 11. According to the IR-9.3.3.6 of the IUPAC recommendations 2005 [35], configuration indices are assigned separately to the enantiomers of each pair by presuming the CIP priority a > b > c > p > $\overline{\text{p}}$.

$$\left.\begin{matrix}\mathbf{161}\ \textit{TBPY-5-44}\\ \overline{\mathbf{161}}\ \textit{TBPY-5-45}\end{matrix}\right\}\ (\mathbf{C}_1)\ \text{Stereoisogram}\ \mathbf{168}\ (\mathbf{D}_{3h\tilde{\sigma}\hat{I}})\ \text{(Type II)}. \tag{79}$$

$$\left.\begin{matrix}\mathbf{174}\ \textit{TBPY-5-13}\\ \overline{\mathbf{174}}\ \textit{TBPY-5-13}\end{matrix}\right\}\ (\mathbf{C}_1)\ \text{Stereoisogram}\ \mathbf{177}\ ((1\ 2)(4\ 5)\mathbf{D}_{3h\tilde{\sigma}\hat{I}})\ \text{(Type II)}. \tag{80}$$

$$\left.\begin{matrix}\mathbf{175}\ \textit{TBPY-5-23}\\ \overline{\mathbf{175}}\ \textit{TBPY-5-23}\end{matrix}\right\}\ (\mathbf{C}_1)\ \text{Stereoisogram}\ \mathbf{178}\ ((1\ 3)(4\ 5)\mathbf{D}_{3h\tilde{\sigma}\hat{I}})\ \text{(Type II)}. \tag{81}$$

$$\left.\begin{matrix}\mathbf{181}\ \textit{TBPY-5-12}\\ \overline{\mathbf{181}}\ \textit{TBPY-5-12}\end{matrix}\right\}\ (\mathbf{C}_1)\ \text{Stereoisogram}\ \mathbf{183}\ ((1\ 2)(3\ 5)\mathbf{D}_{3h\tilde{\sigma}\hat{I}})\ \text{(Type II)}. \tag{82}$$

Note that the two enantiomers of each pair represented by Eqs. 80–82 are not differentiated by means of the assigned configuration indices. The *C/A*-descriptors are not assigned to the respective promolecules (Eqs. 79–82) because of *RS*-astereogenicity (or *RS*-non-stereogenicity) due to the stereoisogram of Type II. In other words, the chirality of each promolecule has nothing to do with the impossibility of giving *C/A*-descriptors.

Even in the case of **161** (Eq. 79), if we separately apply one CIP priority a (1) > b (2) > c (3) > p (4) to **161** with [Mabcp$_2$] and another CIP priority a (1) > b (2) > c (3) > $\overline{\text{p}}$ (4) to $\overline{\mathbf{161}}$ with [Mabc$\overline{\text{p}}_2$], the same configuration index *TBPY-5-44* is given to them. This convention provides us with no reliable way to distinguish such enantiomers of a pair because of the lack of *C/A*-descriptors.

It follows that there are no direct descriptors to distinguish between the central atoms of the respective pairs of enantiomers in the cases of Eqs. 79–82, although the enantiomers of each pair can be distinguished by specifying p and $\overline{\text{p}}$ in terms of *RS*-descriptors.

In summary, the center of **161** (or others collected in Eqs. 79–82) is chiral in a purely geometric meaning, not *RS*-stereogenic (*RS-a*stereogenic, Def. 2), ortho-stereogenic (Def. 1), and stereogenic (Def. 3). The incapability of giving *C/A*-descriptors depends upon the *RS-a*stereogenic property due to Def. 2. The capability of giving stereoisomers depends upon the stereogenicity due to Def. 3 and, more definitely speaking, upon the ortho-stereogenicity due to Def. 1.

The six pairs of chiral promolecules of $\mathbf{C}_1$ are characterized by three stereoisograms of Type III, i.e., Stereoisograms **169**, **170**, and **171**, which exhibit the following coincidence: Stereoisogram **169** ∼ **186**, Stereoisogram **170** ∼ **182**, and Stereoisogram **171** ∼ **176**. According to the IR-9.3.3.6 and IR-9.3.4.5 of the IUPAC recommendations 2005 [35], a pair of configuration indices with a *C/A*-descriptor is assigned to a pair of *RS*-diastereomers (not to a pair of enantiomers) as follows:

162 *TBPY-5-14-A*
163 *TBPY-5-14-C*
$\overline{\textbf{162}}$ *TBPY-5-15-C*
$\overline{\textbf{163}}$ *TBPY-5-15-A*

($\mathbf{C}_1$) Stereoisogram **169** ((1 2)$\mathbf{D}_{3h\widetilde{\sigma}\widehat{I}}$) (Type III) (83)

(equivalent to Stereoisogram **186**)

164 *TBPY-5-24-C*
165 *TBPY-5-24-A*
$\overline{\textbf{164}}$ *TBPY-5-25-A*
$\overline{\textbf{165}}$ *TBPY-5-25-C*

($\mathbf{C}_1$) Stereoisogram **170** ((1 3)$\mathbf{D}_{3h\widetilde{\sigma}\widehat{I}}$) (Type III) (84)

(equivalent to Stereoisogram **182**)

166 *TBPY-5-34-A*
167 *TBPY-5-34-C*
$\overline{\textbf{137}}$ *TBPY-5-35-C*
$\overline{\textbf{138}}$ *TBPY-5-35-A*

($\mathbf{C}_1$) Stereoisogram **171** ((1 4)$\mathbf{D}_{3h\widetilde{\sigma}\widehat{I}}$) (Type III) (85)

(equivalent to Stereoisogram **176**)

It should be noted again that, as found in Eq. 83 for example, the *RS*-diastereomers **162/163** are considered to be pairwise named, i.e., *TBPY-5-14-A* for **162** and *TBPY-5-14-C* for **163**, where the configuration indices (*TBPY-5-14* for both **133** and **134**) are identical with each other and the *C/A*-descriptors are pairwise given. In contrast, if we take account of the enantiomers **162/**$\overline{\textbf{162}}$ by following the conventional stereochemistry, Eq. 83 provides *TBPY-5-14-A* for **162** and *TBPY-5-15-C* for $\overline{\textbf{162}}$, which are not paired because the configuration indices are not identical.

6 Ortho-diastereomeric relationships and enantiomeric ones

The equivalent stereoisograms **141** and **156** shown in Fig. 10 should be examined further from a view point of ortho-stereogenicity. They belong to Type III and are characterized by Eq. 76. The Stereoisogram **141** is converted into Stereoisogram **156** by a permutation (1 5 3) (= (3 5)(1 3)$^{-1}$), which contains no reflection operations. As for the numbering of vertices, see the reference stereoisograms **13** and **28** shown in Fig. 3. It follows that the two stereoisograms are ortho-diastereomeric to each other, if we take account of permutations according to Def. 1. Although they are ortho-diastereomeric to each other, enantiomeric relationships should be examined to demonstrate the equivalency between Stereoisograms **141** and **156**, because a pair of enantiomers has been counted once during the process of symmetry-itemized enumeration shown at the [1,1,1,0,0;1,1,0,0]-row of Table 2.

As found in Fig. 10, the permutation (1 5 3) converts a pair of enantiomers **135/**$\overline{\textbf{135}}$ (in the stereoisogram **141**) into another pair of enantiomers **152/**$\overline{\textbf{152}}$ (in the stereoisogram **156**), which is afterward identified with a pair of $\overline{\textbf{135}}$**/135** during the process of symmetry-itemized enumeration shown at the [1,1,1,0,0;1,1,0,0]-row of Table 2. Although the pair of $\overline{\textbf{135}}$**/135** has the reverse order of appearance in comparison with the pair of **135/**$\overline{\textbf{135}}$ and although the interconversion between the two pairs requires a reflection operation, each of these pairs has been preliminarily paired so that

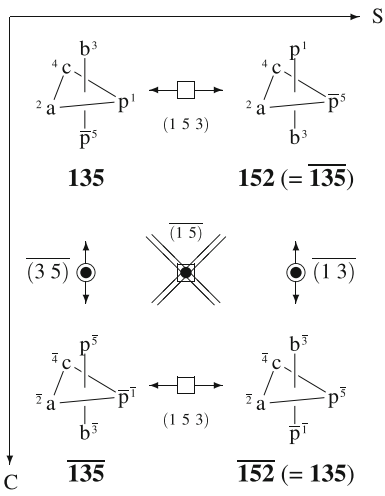

Fig. 12 A skew-stereoisogram for trigonal bipyramidal compounds with *TBPY-5-25-C*- and *TBPY-5-24-A*-[Mabcpp̄] (cf. Fig. 10 and Eq. 76)

these pairs are equalized from a viewpoint of the symmetry-itemized enumeration. By following the process of recognition, we are able to say that the ortho-diastereomeric relationship coincides with the enantiomeric relationship.

To illustrate these conversions, we take account of the left columns of Stereoisograms **141** and **156**, which are collected into a single diagram shown in Fig. 12. The resulting diagram (Fig. 12) is called *a skew-stereoisogram*, where the word "skew" stems from ortho-diastereomeric relationships (denoted by arrows with a box), but not *RS*-diastereomeric relationships.

The coincidence by the ortho-stereogenicity shown in Fig. 12 is seemingly akin to the coincidence in a Type I stereoisogram, which is concerned with an *RS*-diastereomeric relationship (as a pairwise relationship) due to *RS*-stereogenicity. Hence, it is an open problem to determine whether such a permutation operation appearing in a skew-stereoisogram as Fig. 12 (e.g., (1 5 3)) can be regarded as a pairwise relationship or not. At the present time, however, we are safe to presume that the ortho-stereogenicity has nothing to do with the capability of giving *A/C*-descriptors, because an ortho-diastereomeric relationship due to the ortho-stereogenicity is not a pairwise relationship in general. Hence, the capability of giving *A/C*-descriptors should be examined by means of the stereoisogram of Type III (**141** or **156**), where an *RS*-diastereomeric relationship as a pairwise relationship assures the capability of giving *A/C*-descriptors, as shown by Eq. 76.

7 Stereomutation of trigonal bipyramidal compounds

If a trigonal bipyramidal skeleton is so flexible as to cause stereomutation, compounds derived as above from the skeleton should be regarded as configurations participating in the stereomutation. This section is devoted to reinterpretation of Berry's pseudorotation which has been recognized as a standard mechanism of the stereomutation.

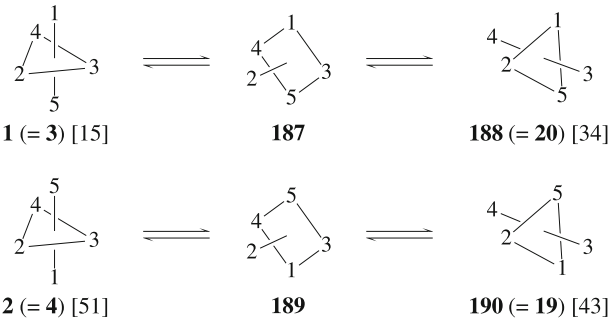

Fig. 13 Pairs interpreted misleadingly as pairs of enantiomers in the conventional interpretation of Berry's pseudorotation. According to the stereoisogram approach, in contrast, each pair of numbering (e.g., **1/2**) is regarded as a pair of *RS*-diastereomers

7.1 Reinterpretation of Berry's pseudorotation

7.1.1 Problematic situations of the conventional interpretation of Berry's pseudorotation

As found in references dealing with Berry's pseudorotation [10,20], the conventional interpretation of Berry's pseudorotation has implicitly presumed that all ligands on a trigonal bipyramidal skeleton are achiral when detached (or simply to be atoms). As a result, a pair of starting configurations in the two processes of Berry's pseudorotation (Fig. 13), i.e., **1/2** (= **3/4**, [15]/[51]) is presumed to be enantiomeric. On the same line, a pair of **188/190** (=**20/19**, [34]/[43]) is presumed to enantiomeric.

Two pairs of digits separated by a slash, e.g., [15]/[51], is used to represent the relationship between trigonal bipyramidal configurations, e.g., **3/4**, where the apical numbers of each configuration of the pair are collected to give a pair of digits, so that the view from a smaller number (e.g., 1) to the larger (e.g., 5) assures the anticlockwise order of the equatorial numbering (e.g., 2–3–4). Thus, the conventional interpretation of Berry's pseudorotation has implicitly presumed that a pair of indices [15]/[51] (or [34]/[43]) represents a pair of enantiomers.

This implicit presumption is seemingly correct so long as all ligands on a trigonal bipyramidal skeleton are achiral when detached (or simply to be atoms). For example, the functions f_1–f_6 (Eqs. 42, 53, 61, 67, 68, and 69) are applied to Fig. 13 so as to give respective pairs of enantiomers. Note that these cases are characterized by stereoisograms of Type I or IV according to the stereoisogram approach.

However, the implicit presumption is misleading if we take account of chiral ligands along with achiral ones. For example, let us apply the function f_7 (Eq. 70) to Fig. 13. Thereby, we obtain pairs of Berry's pseudorotation shown in Fig. 14. Each pair of configurations (e.g., **131/132**) in Fig. 14 is by no means regarded as a pair of enantiomers, even if the two configurations of the pair are represented by the corresponding inverted indices (e.g., [15] and [51]). Note that this case is characterized by stereoisograms of Type V according to the stereoisogram approach, where **131** ([15]) and **132** ([51]) are achiral themselves and they are in an *RS*-diastereomeric relationship (cf. Fig. 10).

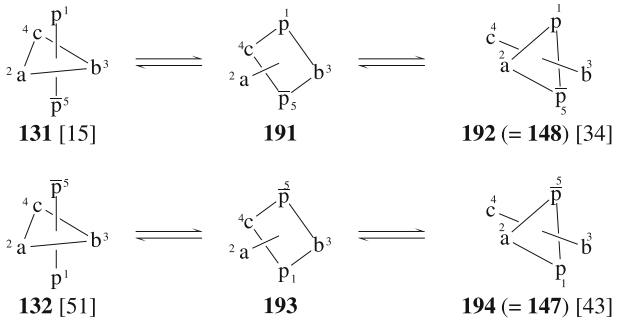

Fig. 14 Pairs of *RS*-diastereomers in Berry's pseudorotation, where they are generated by applying f_7 (Eq. 70) to Fig. 13. Each pair of configurations (e.g., **131/132**) is by no means regarded as a pair of enantiomers

Moreover, there appear no enantiomers if the function f_8 (Eq. 78) is applied to Fig. 13, where the resulting configurations from **1** (= **3**, [15]) and **2** (= **4**, [51]) are in an *RS*-diastereomeric relationship, but not in an enantiomeric relationship (cf. Fig. 11). This is again inconsistent to the implicit presumption that a pair of indices [15]/[51] represents a pair of enantiomers. Note that this case is characterized by stereoisograms of Type II or III according to the stereoisogram approach.

The case of Fig. 14 in inorganic stereochemistry corresponds to so-called pseudoasymmetric cases which have been well-known in organic stereochemistry [48]. We can safely say that the-state-of-the-art interpretation of Berry's pseudorotation does not take account of such pseudoasymmetric cases. More directly speaking, the conventional methodology of inorganic stereochemistry is incapable of treating such pseudoasymmetric cases successfully, just as the conventional methodology of organic stereochemistry has not reached a goal to a successful rationalization of pseudoasymmetric cases.

When we follow the methodology of the stereoisogram approach [25,26,44], the implicit presumption shown by Fig. 13 means the adoption of Type I and IV stereoisograms only and the nullification of Type II, III, and V by the conventional interpretation of Berry's pseudorotation. In particular, a pair of enantiomers treated by the conventional mechanism of Berry's pseudorotation (cf. Fig. 13) should be regarded as a pair of *RS*-diastereomers, if we take account of chiral ligands along with achiral ones, as exemplified by Fig. 14.

7.1.2 Enantiomeric pairs as equivalence classes for Berry's pseudorotation

The terms *stereogenic* and *diastereomeric* (Def. 3), which is defined in place of the conventional terms "stereogenic" and "diastereomeric", provide us a key to reinterpret Berry's pseudorotation, where a pair of enantiomers is treated in the lump as an equivalence class. This idea is applied to the mechanism of Berry's pseudorotation so as to give a scheme shown in Fig. 15. Thus, a pair of enantiomeric reference skeletons of trigonal bipyramidal configurations **1/$\overline{\mathbf{1}}$** (= **3/$\overline{\mathbf{3}}$**) is converted into an intermediate pair of square pyramidal configurations **195/$\overline{\mathbf{195}}$**, which is in turn converted into another pair

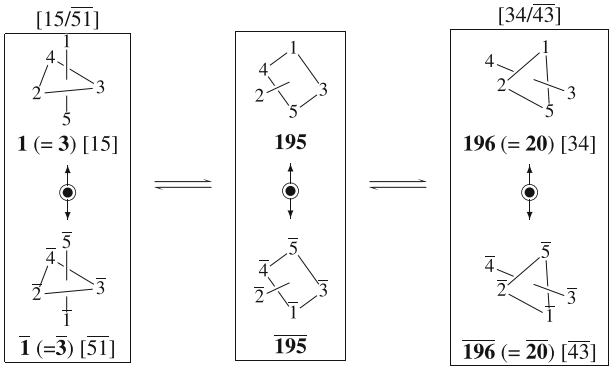

Fig. 15 Reinterpretation of Berry's pseudorotation, with ligand 2 (or $\overline{2}$) serving as pivot. A double-headed arrow may be changed into an equality symbol if self-enantiomeric (i.e., achiral)

of trigonal bipyramidal configurations **196/$\overline{196}$** (= **20/$\overline{20}$**). Note that this conversion is based on the selection of ligand 2 (or $\overline{2}$) serving as pivot.

According to Def. 3, the pair of **1/$\overline{1}$** (= **3/$\overline{3}$**) and the pair of **196/$\overline{196}$** (= **20/$\overline{20}$**) are in a diastereomeric relationship. According to Def. 1, these pairs are in an ortho-diastereomeric relationship. According to Def. 2, these pairs are not in an *RS*-diastereomeric relationship.

A pair of digits and its overlined counterpart separated by a slash, e.g., [15/$\overline{51}$], is used to represent a pair of enantiomers, e.g., **3/$\overline{3}$**, where the apical numbers of each compound of the pair are collected to give a pair of digits, so that the view from a smaller number (e.g., 1) to the larger (e.g., 5) assures the anticlockwise order of the equatorial numbering (e.g., 2–3–4). Thereby the process shown in Fig. 15 is represented as [15/$\overline{51}$] $\rightleftharpoons$ [34/$\overline{43}$].

7.1.3 Modification of the Desargues-Levi graph

On the same line as Fig. 15, a pair of enantiomeric reference skeletons selected from Fig. 3 is converted into one of the remaining 19 pairs of enantiomeric reference skeletons, where a pair of digits and its overlined counterpart (e.g., [15/$\overline{51}$]) is attached to the top of each pair (e.g., **3/$\overline{3}$** (= **1/$\overline{1}$**)). The whole conversion processes are represented by a Desargues-Levi graph (Fig. 16 left), where each node corresponds to a pair of enantiomeric reference skeletons (Fig. 3), which is denoted by a index such as [15/$\overline{51}$]. Note that the pair of enantiomers at an appropriate node (e.g., [15/$\overline{51}$]) is accompanied by the corresponding pair of enantiomers (e.g., [51/$\overline{15}$]), where they are in an *RS*-diastereomeric relationship, as exemplified in the right of Fig. 16 (cf. Fig. 2).

The point group $\mathbf{D}_{3h}$ ($|\mathbf{D}_{3h}| = 12$) for characterizing a pair of enantiomeric trigonal bipyramidal skeletons is a subgroup of the stereoisomeric group $\mathbf{S}^{[5]}_{\mathbf{D}_{3h\tilde{\sigma}\hat{I}}}$ ($|\mathbf{S}^{[5]}_{\mathbf{D}_{3h\tilde{\sigma}\hat{I}}}| = 240$) shown in Eq. 32. The orbit (equivalence class) of such pairs of enantiomeric trigonal bipyramidal skeletons is governed by the coset representation $\mathbf{S}^{[5]}_{\mathbf{D}_{3h\tilde{\sigma}\hat{I}}}(/\mathbf{D}_{3h})$, the degree of which is calculated as follows:

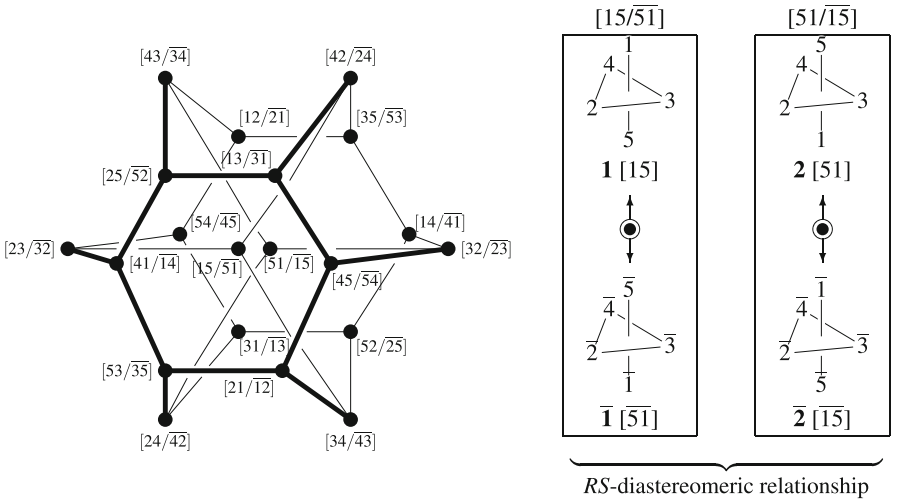

Fig. 16 Modified Desargues-Levi graph based on pairs of enantiomers (*left*), where each pair of enantiomeric reference skeletons selected from Fig. 3 is placed at an appropriate node. The nodes linked by a line can be converted into each other by Berry's pseudorotation. A pair of enantiomers at an appropriate node is *RS*-diastereomeric or ortho-diastereomeric (or diastereomeric) to a pair of enantiomers of another node. An example of pairs in an *RS*-diastereomeric relationship is shown in the *right* diagram

$$\frac{|\mathbf{S}^{[5]}_{\mathbf{D}_{3h}\widehat{\sigma}\widehat{I}}|}{|\mathbf{D}_{3h}|} = \frac{240}{12} = 20. \tag{86}$$

This shows the number of vertices of the modified Desargues-Levi graph (Fig. 16).

To draw a modified Desargues-Levi graph for trigonal bipyramidal configurations with a given constitution (e.g., [Mabcde]), the corresponding function (e.g., f_1 represented by (Eq. 42) is applied to the left of Fig. 16 by referring to the multiplet of stereoisograms shown by Fig. 3. As for the constitution [Mabcde], each pair of enantiomers appearing in the multiplet shown by Fig. 4 is placed on an appropriate node of the left of Fig. 16 by referring to such an index as [51/$\overline{15}$].

In similar ways, the applications of f_2–f_6 (Eqs. 53, 61, 67, 68, and 69) to Fig. 13 generate the modified Desargues-Levi graphs of respective constitutions, where respective nodes are occupied by pairs of enantiomers selected from the corresponding multiplets of stereoisograms (Figs. 5–9). Note that a double-headed arrow is changed into an equality symbol if self-enantiomeric (i.e., achiral).

In the modified Desargues-Levi graphs corresponding to the multiplets of stereoisograms of Type I or Type IV (Figs. 4–9), a pair of enantiomers such as [15/$\overline{51}$] and a pair of enantiomers such as [51/$\overline{15}$], which are in a *RS*-diastereomeric relationship, are degenerated into a pair of enantiomers. It follows that the notations [15] (in place of [15/$\overline{51}$]) and [51] (in place of [51/$\overline{15}$]) are conventionally used to refer to a pair of enantiomers (cf. the caption of Fig. 2 (a diagram of the Desargues-Levi Graph) in [10]). However, the full notations [15/$\overline{51}$] and [51/$\overline{15}$] should be used to treat extended cases of Type II, III, and V cases, as mentioned in the next paragraph.

In cases of constitutions containing chiral proligands along with achiral ones, the corresponding modified Desargues-Levi graphs are drawn similarly. For example,

the applications of f_7 (Eq. 70) and f_8 (Eqs. 78) to Fig. 13 generate the modified Desargues-Levi graphs, where respective nodes are occupied by pairs of enantiomers selected from the corresponding multiplets of stereoisograms (Figs. 10 and 11). Thus, the 20 nodes of Fig. 16 are remained in the modified Desargues-Levi graph generated by the function f_7 (Eq. 70). Among them, 12 pairs of enantiomers (due to the six stereoisograms of Type III in Fig. 10) on the 12 nodes are ortho-diastereomeric so as to give six skew-stereoisograms (cf. Fig. 12), which correspond to six pairs of enantiomers of $\mathbf{C}_1$ because of the coincidence between ortho-diastereomeric relationships and enantiomeric relationships. As for 8 achiral configurations (due to the four stereoisogram of Type V in Fig. 10) on the 8 nodes, the notations of nodes, i.e., [15/$\overline{51}$], [51/$\overline{15}$]; [42/$\overline{24}$], [24/$\overline{42}$]; [34/$\overline{43}$], [43/$\overline{34}$]; [23/$\overline{32}$], and [32/$\overline{23}$], are changed into A[15] (**131**), A[51] (**132**); A[42] (**145**), A[24] (**146**); A[34] (**148**), A[43] (**147**); A[23] (**155**), and A[32] (**154**), which represent achiral configurations. These changes (e.g., [15/$\overline{51}$], [51/$\overline{15}$] into A[15], A[51]) indicate, again, that each pair of nodes in Fig. 16 (a pair of [15/$\overline{51}$] and [51/$\overline{15}$] etc. separated by a semicolon) does not represent a pair of enantiomers but a pair of *RS*-diastereomers.

It is emphasized again that the modified Desargues-Levi graph shown in Fig. 16 is based on the scheme of Fig. 15, but not on the scheme of Fig. 13. The reinterpretation of Berry's pseudorotation in terms of the scheme of Fig. 15 stems from the recognition that the pair of [15] and [51] does not represent a pair of enantiomers, but a pair of *RS*-diastereomers. This recognition is essential to comprehend stereochemistry, even though the pair of [15] and [51] may coincide with an pair of enantiomers if only achiral ligands are taken into consideration. In particular, compare the modified Desargues-Levi graph for the constitution [Mabcde] by f_1 (Eq. 42) with the counterpart for the constitution [Mabcp$\overline{\text{p}}$] by f_7 (Eq. 70). These two cases provide us with a typical example which should be interpreted in a common theoretical foundation based on the recognition. Hence, for the sake of stricter discussions, full notations such as [15/$\overline{51}$] and [51/$\overline{15}$] are required to characterize the nodes of the modified Desargues-Levi graph (Fig. 16), because chiral ligands along with achiral ones should be taken into consideration.

In addition, the term *diastereomeric* defined by Def. 3 is permissible to refer to the *RS*-diastereomeric relationship between [15/$\overline{51}$] and [51/$\overline{15}$], if our discussions are intended to be harmonized with the conventional terminology of inorganic stereochemistry. This course inevitably forces us to change the connotation of the dichotomy between enantiomers and diastereomers, as already pointed out by us [49].

7.2 Interpretation of Berry's pseudorotation by stereoisograms

7.2.1 Stereoisograms for interpreting Berry's pseudorotation

The viewpoint introduced by Fig. 15 is further sophisticated by considering stereoisograms. For the sake of simplicity, let us introduce a notation $Q[v_1 v_2]$ for indicating a stereoisogram. The notation $Q[v_1 v_2]$ indicates a stereoisogram in which a representative promolecule at the upperleft position of the stereoisogram, where the view from the number of the first apical vertex (v_1) to that of the second one (v_2) assures the

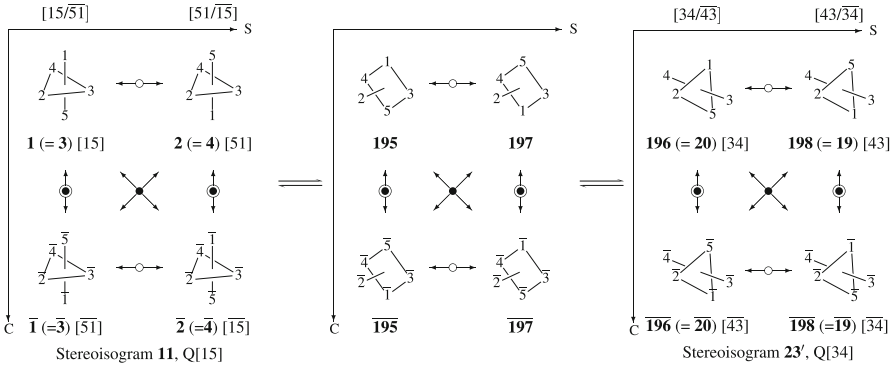

Fig. 17 Stereoisograms for interpreting Berry's pseudorotation, with ligand 2 (or $\overline{2}$) serving as pivot. A set of stereoisograms of Type III may be changed into a set of Stereoisograms of Type I—V

anticlockwise order of the equatorial numbering. These notations are used to differentiate the stereoisograms collected in Fig. 3. Note that a stereoisogram represented by the notation $Q[v_1v_2]$ contains a quadruplet of *RS*-stereoisomers denoted by $[v_1v_2]$, $[\overline{v_2v_1}]$, $[v_2v_1]$, and $[\overline{v_1v_2}]$, which are categorized into two pairs of enantiomers denoted by $[v_1v_2/\overline{v_2v_1}]$ and $[v_2v_1/\overline{v_1v_2}]$.

The scheme of Fig. 15 for a pair of enantiomers is extended by considering a *RS*-diastereomeric relationship shown in the right of Fig. 16 so as to give Fig. 17 for quadruplets of *RS*-stereoisomers, where an equatorial proligand at each vertex 2 is selected as a pivot. By following the newly-defined notation, Fig. 17 shows that the quadruplet $Q[15]$ (i.e., Stereoisogram **11**) is converted into another quadruplet $Q[34]$ (i.e., Stereoisogram **23**′). Note that Stereoisogram **23**′ (a representative promolecule **20**, [34]) is generated by changing the representative promolecule (**19**, [43]) of Stereoisogram **23**, which is denoted by $Q[43]$ as found in Fig. 3. Such a stereoisogram as having a number with a prime is called "an exchanged counterpart", which indicates the exchange of columns of a stereoisogram to select a representative promolecule. It should be noted, however, that $Q[v_1v_2]$ and $Q[v_2v_1]$ represent the same quadruplet of *RS*-stereoisomers, although the corresponding stereoisograms (denoted by numbers without or with a prime) suffer from the exchange of the columns.

7.2.2 Adamantane-like graphs for interpreting Berry's pseudorotation

In similar ways to the conversion ($Q[15] \rightarrow Q[34]$) shown in Fig. 17 (due to the pivot 2), the selection of the other equatorial vertex 3 or 4 as a pivot causes another conversion $Q[15] \rightarrow Q[23]$ (i.e., Stereoisogram **29**′) or $Q[15] \rightarrow Q[42]$ (i.e., Stereoisogram **22**′). Obviously, such a conversion is generally represented by a scheme:

$$Q[v_1v_2] \xrightarrow[v_3]{\text{pivot}} Q[v_4v_5], \tag{87}$$

where the numbers v_1–v_5 are selected one by one from 1 to 5 without duplication. Examination of processes of such Berry's pseudorotation generates an adamantane-like graph **199** shown in Fig. 18 (left), in which each node accommodates

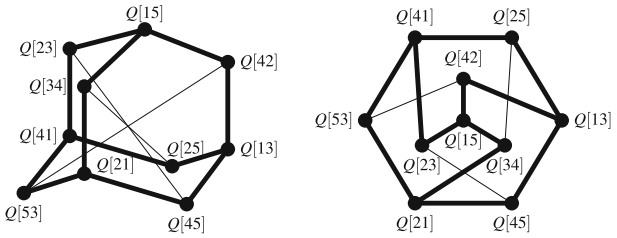

Fig. 18 Adamantane-like graph based on quadruplets of *RS*-stereoisomers of trigonal bipyramidal skeletons (*left*) and an equivalent graph of connectivity 3 and diameter 2 (*right*)

a quadruplet of *RS*-stereoisomers denoted by the notation $Q[v_1 v_2]$. For the corresponding stereoisograms, see Fig. 3. As a planar representation of the adamantane-like graph, Fig. 18 (right) shows an equivalent graph **200** of connectivity 3 and diameter 2.

The vertical thick lines of the adamantane-like graph **199** correspond to the following processes of Berry's pseudorotation:

$$Q[42] \underset{5}{\overset{\text{pivot}}{\rightleftharpoons}} Q[13] \tag{88}$$

$$Q[23] \underset{5}{\overset{\text{pivot}}{\rightleftharpoons}} Q[41] \tag{89}$$

$$Q[34] \underset{5}{\overset{\text{pivot}}{\rightleftharpoons}} Q[21], \tag{90}$$

where the vertex 5 is selected as a common pivot. The resulting quadruplets of *RS*-stereoisomers ($Q[13]$, $Q[41]$, and $Q[21]$) correspond to Stereoisograms **28**′, **21**′, and **32**′, the exchanged counterparts of which are collected in the first column of Fig. 3. They have vertex 1 as a common apical vertex, just as the starting stereoisogram $Q[15]$ at the top of the first column has an apical vertex 1. Note that the first column of Fig. 3 contains all of the stereoisograms having the vertex 1 as an apical vertex.

After the thick-line processes are selected as shown in the adamantane-like graph **199**, the thin-line processes require the changing of the representative promolecule:

$$Q[42] \underset{1}{\overset{\text{pivot}}{\rightleftharpoons}} Q[35] \tag{91}$$

$$Q[23] \underset{1}{\overset{\text{pivot}}{\rightleftharpoons}} Q[54] \tag{92}$$

$$Q[34] \underset{1}{\overset{\text{pivot}}{\rightleftharpoons}} Q[52], \tag{93}$$

where the vertex 1 is selected as a common pivot. Note that the quadruplets of *RS*-stereoisomers, $Q[35]$, $Q[54]$, and $Q[52]$, are regarded as being equivalent to $Q[53]$, $Q[45]$, and $Q[25]$ shown in the adamantane-like graph **199**.

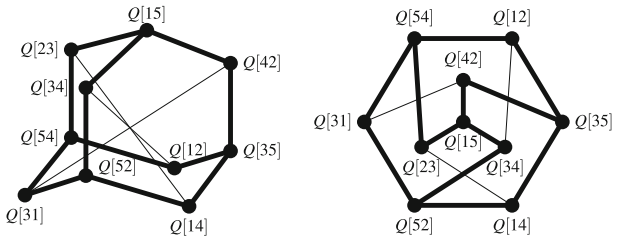

Fig. 19 Another adamantane-like graph based on quadruplets of *RS*-stereoisomers of trigonal bipyramidal skeletons (*left*) and an equivalent graph of connectivity 3 and diameter 2 (*right*)

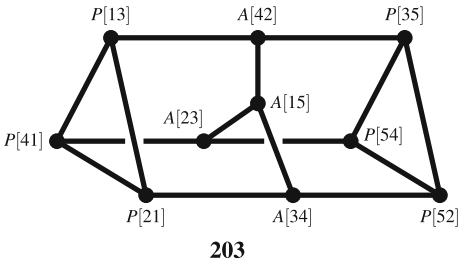

Fig. 20 Correlation graph based on pairs of enantiomers with [Ma_2bcd], which are collected in Fig. 5. The symbols $A[v_1 v_2]$ (for an achiral compound) and $P[v_1 v_2]$ (for a pair of enantiomers) at respective nodes denote modes of degeneration shown in Table 4

On the other hand, when the common pivot 5 for Eqs. 88–90 are changed into the vertex 1, there emerge the conversions shown by Eqs. 91–93. Thereby, another adamantane-like graph **201** (or an equivalent planar graph **202**) is generated as shown in Fig. 19, where the resulting quadruplets $Q[35]$, $Q[54]$, and $Q[52]$ correspond to Stereoisograms **13**′, **14**′, and **11**′, the exchanged counterparts of which are collected in the first row of Fig. 3. Note that the first row of Fig. 3 contains all of the stereoisograms having the vertex 5 as an apical vertex. The thin-line processes in Fig. 19 require the changing of the representative promolecule represented by Eqs. 88–90.

7.3 Pairs of enantiomers versus quadruplets of *RS*-stereoisomers

The full aspect of the modified Desargues-Levi graph is found for for the constitution [Mabcde] by f_1 (Eq. 42), where the 20 nodes of the graph represent inequivalent pairs of enantiomeric compounds or configurations.

On the other hand, other functions exhibit restricted aspects according to their constitutions. For example, the compounds or configurations with [Ma_2bcd] collected in Fig. 5 correspond to a correlation graph **203** shown in Fig. 20, which is generated by the degeneration of the nodes in the modified Desargues-Levi graph (Fig. 16).

The resulting nodes in the graph **203** are categorized into two kinds. The symbol $A[v_1 v_2]$ indicates that the resulting node is concerned with an achiral compound, while the symbol $P[v_1 v_2]$ indicates that the resulting node is concerned with a pair of enantiomers.

The nodes of the correlation graph (**203** of Fig. 20) denote respective modes of degenerations shown in Table 4. The equality symbol in $[15/\overline{51}] = [51/\overline{15}]$ at the

Table 4 Nodes of the correlation diagram **203** shown in Fig. 20 for the constitution [Ma_2bcd]

Node	Pairs of enantiomers	Compound no.	Assignment	Quadruplet
A[15]	[15/$\overline{51}$] = [51/$\overline{15}$]	**63**	Eq. 57	Q[15] (Type IV)
A[42]	[42/$\overline{24}$] = [24/$\overline{42}$]	**76′**	Eq. 54	Q[42] (Type IV)
A[34]	[34/$\overline{43}$] = [43/$\overline{34}$]	**77′**	Eq. 55	Q[34] (Type IV)
A[23]	[23/$\overline{32}$] = [32/$\overline{23}$]	**83′**	Eq. 56	Q[23] (Type IV)
P[21]	[21/$\overline{12}$] ∼ [25/$\overline{52}$]	**87/$\overline{87}$** ∼ **64/$\overline{64}$**	Eq. 58	Q[21](∼ Q[25]) (Type I)
P[52]	[52/$\overline{25}$] ∼ [12/$\overline{21}$]	**65/$\overline{65}$** ∼ **86/$\overline{86}$**		
P[13]	[13/$\overline{31}$] ∼ [53/$\overline{35}$]	**82/$\overline{82}$** ∼ **66/$\overline{66}$**	Eq. 59	Q[13](∼ Q[53]) (Type I)
P[35]	[35/$\overline{53}$] ∼ [31/$\overline{13}$]	**67/$\overline{67}$** ∼ **81/$\overline{81}$**		
P[41]	[41/$\overline{14}$] ∼ [45/$\overline{54}$]	**75/$\overline{75}$** ∼ **68/$\overline{68}$**	Eq. 60	Q[41](∼ Q[45]) (Type I)
P[54]	[54/$\overline{45}$] ∼ [14/$\overline{41}$]	**69/$\overline{69}$** ∼ **74/$\overline{74}$**		

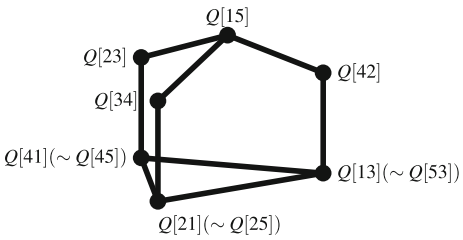

204

Fig. 21 Correlation graph based on quadruplets of *RS*-stereoisomers with [Ma_2bcd], which are collected in Fig. 5, where each quadruplet is denoted by the notation $Q[v_1 v_2]$

A[15]-row, for example, represents degeneration into a single achiral compound, as found for the compound **63** which is characterized by Eq. 57. The other achiral compounds characterized by Eqs. 54–56 appear as nodes.

The symbol ∼ in [21/$\overline{12}$] ∼ [25/$\overline{52}$] at the P[21]-row of Table 4, for example, indicates that a pair of enantiomers [21/$\overline{12}$] is equivalent to another pair of enantiomers [25/$\overline{52}$], as found for the equivalency between a pair of **87/$\overline{87}$** and another pair of **64/$\overline{64}$** (Eq. 58). The nodes P[21] and P[52], each of which is a pair of enantiomers, are in an *RS*-diastereomeric relationship, as combined with a brace. The remaining two pairs of *RS*-diastereomers, each of which is combined with a brace, are also shown in Table 4.

From the viewpoint of the stereoisogram approach, the full aspect of the adamantane-like graph (Fig. 18) is accomplished by the constitution [Mabcde] by f_1 (Eq. 42) where the 10 nodes correspond to inequivalent quadruplets of *RS*-stereoisomers.

The other functions described above exhibit restricted aspects according to their constitutions. For example, the compounds with [Ma_2bcd] collected in Fig. 5 correspond to a correlation graph shown in Fig. 21, where the resulting nodes are characterized by the notation $Q[v_1 v_2]$.

The symbol ∼ in Q[13](∼ Q[53]), for example, indicates that a quadruplet Q[13] is equivalent to another quadruplet Q[53], as found for the equivalency between Stereoisogram **72** and Stereoisogram **84** (Eq. 59). The resulting node Q[13] (∼ Q[53])

in **204** (Fig. 21) corresponds to a pair of $P[13]/P[35]$ in **203** (Fig. 20), as shown in the "quadruplet"-column of Table 4. Thus, the three pairs denoted by $P[21]/P[52]$, $P[13]/P[35]$, and $P[41]/P[54]$ in Fig. 20 are degenerated respectively into the nodes denoted by $Q[21]$, $Q[13]$, and $Q[41]$ in Fig. 21, which are characterized as stereoisograms of Type I. On the other hand, the four nodes denoted by $A[15]$, $A[42]$, $A[34]$, and $A[23]$ in **203** (Fig. 20) correspond respectively to the nodes denoted by $Q[15]$, $Q[42]$, $Q[34]$, and $Q[23]$ in **204** (Fig. 21) without exhibiting degeneration, where these are characterized as stereoisograms of Type IV.

The comparison between Figs. 20 and 21 reveals the difference between the methodology based on pairs of enantiomers and the methodology based on quadruplets of *RS*-stereoisomers. The former graph **203** contains two kinds of nodes, i.e., $A[v_1v_2]$ and $P[v_1v_2]$, while the latter graph **204** contains a single kind of nodes, i.e., $Q[v_1v_2]$. It should be emphasized again that chirality and *RS*-stereogenicity (e.g., *C/A*-descriptors) can be discussed in terms of a stereoisogram which consists of *RS*-stereoisomers of a quadruplet denoted by the symbol $Q[v_1v_2]$.

8 Conclusions

The stereoisogram approach [25–32] is applied to trigonal bipyramidal compounds, where chiral and achiral proligands are taken into consideration.

1. Configurations of trigonal bipyramidal compounds are enumerated by using the PCI method of the the USCI approach [33], where both chiral and achiral proligands are taken into consideration.
2. Enumerated configurations are categorized into Type I–V cases according to the stereoisogram approach. It is clarified that the conventional stereochemistry has discussed Type I and IV cases and ignored Type II, III, and V cases among the five cases, because only achiral proligands are taken into consideration.
3. Enumerated configurations are specified by configuration indices and *C/A*-descriptors according to the IR-9.3.3.6 and IR-9.3.4.5 of the IUPAC recommendations 2005 [35]. *C/A*-Descriptors are clarified to be based on *RS*-stereogenicity (due to stereoisograms of Type I, III, and V), but not on chirality (due to stereoisograms of Type I, II, and III). Thereby, the rules based on the conventional presumption that a pair of *C/A*-descriptors is assigned to a pair of enantiomers are reinterpreted to be assigned to a pair of *RS*-diastereomers (not to a pair of enantiomers).
4. The concept of *a multiplet of stereoisograms* is proposed to formulate the concept of *ortho-stereogenicity*, which is concerned with *ortho-diastereomeric relationships* between stereoisograms. On the other hand, the concept of *stereogenicity* (which has been used in the conventional stereochemistry) is redefined by starting from *RS*-stereogenicity and by comparing with the ortho-stereogenicity, where the stereogenicity is concerned with *diastereomeric relationships* between pairs of enantiomers.
5. Berry's pseudorotation [1] is reinterpreted in order to cover more general cases in which chiral moieties along with achiral moieties (i.e., all of Type I–V cases) are taken into consideration. A modified Desargues-Levi graph is proposed to cover Type I–V cases.

6. Berry's pseudorotation is remodelled on the basis of stereoisograms, so as to propose an adamantane-like graph which is concerned with quadruplets of *RS*-stereoisomers. Thereby, a multiplet of stereoisograms is shown to be a versatile tool to characterize stereoisomerization processes.

References

1. R.S. Berry, J. Chem. Phys. **32**, 933–938 (1960)
2. E.L. Muetterties, J. Am. Chem. Soc. **91**, 1636–1643 (1969)
3. E.L. Muetterties, J. Am. Chem. Soc. **91**, 4115–4122 (1969)
4. I. Ugi, D. Marquarding, H. Klusacek, P. Gillespie, F. Ramirez, Acc. Chem. Res. **4**, 288–296 (1971)
5. J. Brocas, M. Gielen, R. Willem, *The Permutational Approach to Dynamic Stereochemistry* (McGraw-Hill International, New York, 1983)
6. I. Ugi, J. Dugundji, R. Kopp, D. Marquarding, *Perspectives in Theoretical Stereochemistry* (Springer, Berlin, 1984)
7. J.S. Wood, Prog. Inorg. Chem. **16**, 227–486 (1972)
8. I. Ugi, Chimia **40**, 340–350 (1986)
9. IUPAC Organic Chemistry Division, Pure Appl. Chem. **68** 2193–2222 (1996)
10. R. Engel, J.I. Rizzo, Curr. Org. Chem. **10**, 2393–2405 (2006)
11. K.C.K. Swamy, N.S. Kumar, Acc. Chem. Res. **39**, 324–333 (2006)
12. P.C. Lauterbur, F. Ramirez, J. Am. Chem. Soc. **90**, 6722–6726 (1968)
13. A.T. Balaban, D. Farcasiu, R. Banica, Rev. Roum. Chim. **11**, 1205–1227 (1966)
14. A.T. Balaban, J. Chem. Inf. Model. **35**, 339–350 (1995)
15. K.E. DeBruin, K. Naumann, G. Zon, K. Mislow, J. Am. Chem. Soc. **91**, 7031–7040 (1969)
16. K. Mislow, Acc. Chem. Res. **3**, 321–331 (1970)
17. M. Randić, Int. J. Quantum Chem. **15**, 663–682 (1979)
18. M. Randić, V. Katović, Int. J. Quantum Chem. **21**, 647–663 (1982)
19. E.P.A. Couzijn, J.C. Slootweg, A.W. Ehlers, K. Lammertsma, J. Am. Chem. Soc. **132**, 18127–18140 (2010)
20. C. Moberg, Angew. Chem. Int. Ed. Engl. **50**, 10290–10292 (2011)
21. D. Hellwinkel, Chem. Ber. **99**, 3642–3667 (1966)
22. S. Kojima, K. Kajiyam, K. Akiba, Tetrahedron Lett. **35**, 7037–7040 (1994)
23. J.-B. Hou, H. Zhang, J.-N. Guo, Y. Liu, P.-X. Xu, Y.-F. Zhao, G.M. Blackburn, Org. Biomol. Chem. **7**, 3020–3023 (2009)
24. G. Yang, Y. Xu, J. Hou, H. Zhang, Y. Zhao, Dalton Trans. **39**, 6953–6959 (2010)
25. S. Fujita, J. Org. Chem. **69**, 3158–3165 (2004)
26. S. Fujita, J. Math. Chem. **35**, 265–287 (2004)
27. S. Fujita, MATCH Commun. Math. Comput. Chem. **52**, 3–18 (2004)
28. S. Fujita, MATCH Commun. Math. Comput. Chem. **61**, 11–38 (2009)
29. S. Fujita, Tetrahedron **62**, 691–705 (2006)
30. S. Fujita, Tetrahedron **65**, 1581–1592 (2009)
31. S. Fujita, J. Comput. Aided Chem. **10**, 16–29 (2009)
32. S. Fujita, J. Math. Chem. **49**, 95–162 (2011)
33. S. Fujita, *Symmetry and Combinatorial Enumeration in Chemistry* (Springer, Berlin, 1991)
34. S. Fujita, Bull. Chem. Soc. Jpn. **63**, 1876–1883 (1990)
35. N.G. Connelly, T. Damhus, R.M. Hartshorn, A.T. Hutton, *Nomenclature of Inorganic Chemistry. IUPAC Recommendations 2005* (The Royal Society of Chemistry, Cambridge, 2005)
36. S. Fujita, Theor. Chim. Acta **76**, 247–268 (1989)
37. S. Fujita, J. Math. Chem. **5**, 121–156 (1990)
38. S. Fujita, Bull. Chem. Soc. Jpn. **63**, 203–215 (1990)
39. S. Fujita, J. Math. Chem. **12**, 173–195 (1993)
40. S. Fujita, Bull. Chem. Soc. Jpn. **73**, 329–339 (2000)
41. S. Fujita, Theor. Chim. Acta **82**, 473–498 (1992)
42. S. Fujita, Bull. Chem. Soc. Jpn. **63**, 315–327 (1990)
43. S. Fujita, Tetrahedron **47**, 31–46 (1991)

44. S. Fujita, Tetrahedron **60**, 11629–11638 (2004)
45. A. von Zelewsky, *Stereochemistry of Coordination Compounds* (Wiley, Chichester, 1996)
46. E.L. Eliel, S.H. Wilen, *Stereochemistry of Organic Compounds* (Wiley, New York, 1994)
47. E.L. Eliel, S.H. Willen, M.P. Doyle, *Basic Organic Stereochemistry* (Wiley-Interscience, New York, 2001)
48. V. Prelog, G. Helmchen, Helv. Chim. Acta **55**, 2581–2598 (1972)
49. S. Fujita, in Carbon Bonding and Structures. Advances in Physics and Chemistry, ed. by M.V. Putz, (Springer, Dordrecht, 2011), vol. 5 of Carbon Materials: Chemistry and Physics, Chapter 10, pp. 227–271